TABLE 2 The distance between two terminal atoms in the side chain of the seventh amino acid, Asp (D) within epitope peptide and atoms in main chain of the nearest portion within the TCR

	N (S28)	C_α (S28)	C (S28)	O (S28)	N (Q29)	C_α (Q29)	C (Q29)	O (Q29)	N (Y30)	C_α (Y30)	C (Y30)	O (Y30)
OD1	10.86	9.55	8.37	7.24	8.76	7.98	7.60	6.99	8.27	8.39	8.29	9.37
OD2	8.83	7.48	6.40	5.24	6.97	6.44	6.21	5.91	6.76	7.08	6.84	7.88

Unit of the distance is Å. The values are calculated using 1kj2 (PDB code), which is TCR/peptide/ MHC complex structure obtained from x-ray crystallographic analysis. The OD1 or OD2 represents the terminal atom of the side chain in the seventh amino acid, aspaltic acid (D), within epitope peptide pKB1(aa: KVITFIDL). The amino acids Ser 28 (S28), Gln 29 (Q29), and Tyr 30 (Y30) are the nearest portion within the TCR from the OD1 or OD2.

structure, except for the hydrogen atoms, if one terminal carbon atom of the side chain of V is exchanged for one oxygen atom. According to the quantum chemical calculation, the net charge of the carbon or the oxygen is −0.3e or −0.4e, respectively. In addition, three hydrogen atoms, which have positive charges, are added to the carbon, whereas one hydrogen atom is added to the oxygen. Thus, T generates a greater negative net charge than V. The influence of this charge difference was evident when LINE-IIIB recognized the peptide. It is likely that T had a greater repulsive force against the oxygen atoms in the CDR1 loop compared with V. This repulsive force may account for the significant reduction in the recognition by LINE-IIIB after substitution with T. These findings indicate that the charge of an amino acid at a specific position within an epitope can affect its binding capacity to MHC molecules and/or the interaction with a TCR.

Although the method we applied here for modeling the TCR/peptide/class I MHC complex was not directly based on crystallographic analysis, our computer-based molecular modeling was still accurate. Indeed, as demonstrated in Fig. 7, the predicted 3D structure for 1dn0D by MODELLER was similar to that determined experimentally, and the core regions appeared to be nearly identical. This reflects the fact that the 3D structures of the core regions of the TCR consist of a four-stranded antiparallel β-sheet and a three-stranded anti-parallel β-sheet linked by a disulfide bond. Although the predicted 3D structure of CDR3 seems slightly different from the experimental 3D structure of CDR3 because of the large loop, the predicted 3D structure of CDR1 appears almost the same as the experimental 3D structure. These results suggest that the TCR domain predicted by the present molecular modeling methods can become useful and reliable tools for the structural analysis of TCRs.

TABLE 3 The distance between two terminal atoms in the side chain of 325V or 325v and atoms in main chain of the obtained TCR-CDR1 through molecular modeling

	Vβ7	N(S)	Cα(S)	C(S)	O(S)	N(H)	Cα(H)	C(H)	O(H)
1a6wH	CG1(325V)	10.20	9.55	8.56	8.52	7.99	7.08	7.85	7.48
	CG2(325V)	9.57	8.88	7.62	7.41	7.01	5.80	6.17	5.57
1dn0D	CG1(325V)	10.03	9.43	8.73	8.11	9.12	8.90	9.30	9.33
	CG2(325V)	9.40	8.79	7.77	6.99	8.06	7.58	7.65	7.48
1tcrA	CG1(325V)	7.69	6.38	6.49	7.45	5.86	6.44	7.84	8.34
	CG2(325V)	6.63	5.41	5.09	5.76	4.51	4.80	6.29	6.97
1ao7D	CG1(325V)	7.57	6.48	7.18	6.85	8.40	9.21	9.59	10.11
	CG2(325V)	6.91	5.63	5.85	5.34	6.96	7.48	7.89	8.63
1kb5A	CG1(325V)	7.51	8.02	7.58	6.44	8.67	8.81	9.71	10.44
	CG2(325V)	6.77	7.06	6.21	4.99	7.08	6.92	7.89	8.79
1a6wH	CG1(325v)	8.10	7.48	6.70	6.85	6.20	5.60	6.69	6.63
	CG2(325v)	6.95	6.27	5.12	5.09	4.53	3.56	4.38	4.18
1dn0D	CG1(325v)	7.94	7.34	6.88	6.41	7.39	7.47	8.10	8.42
	CG2(325v)	6.79	6.16	5.28	4.59	5.73	5.59	5.91	6.14
1tcrA	CG1(325v)	6.51	5.12	5.35	6.50	4.59	5.40	6.57	6.84
	CG2(325v)	5.01	3.61	3.26	4.28	2.35	3.02	4.34	4.78
1ao7D	CG1(325v)	5.64	4.73	5.73	5.63	6.98	8.02	8.36	8.66
	CG2(325v)	4.39	3.09	3.63	3.36	4.88	5.73	6.12	6.61
1kb5A	CG1(325v)	5.60	6.21	6.12	5.18	7.37	7.86	8.74	9.24
	CG2(325v)	4.21	4.55	4.02	2.91	5.16	5.49	6.49	7.13

Unit of the distance is Å. The code 1a6wH, 1dn0D, 1tcrA, 1ao7D, or 1kb5A represents each template protein to determine the structure of Vβ7. CG1 and CG2 are two terminal atoms of side chain in 325V or 325v. The successive two amino acids, Ser and His, within CDR1 of Vβ7 are the nearest portion for CG1 or CG2.

In these sorts of structural analyses, it should be acknowledged that a substitution of D-valine (v) for L-valine (V) would result in a conformational interference between the class I MHC molecule and the D-valine (v), which itself could decrease the recognition response by LINE-IIIB. However, as shown in Fig. 9, no conformational interference occurred in this study. Thus, I10(325v) would also be associated with the class I MHC molecule so that TCRs may recognize the epitope. Therefore, our findings suggest that the change in the recognition response by LINE-IIIB after the D-valine (v) substitution reflects the interaction with the TCR.

Our molecular modeling analysis demonstrated that the critical area of the TCR for interacting with 325V within P18-I10 was the peptide DMSHET, within the CDR1 of Vβ7. In contrast, the substituted peptide with the D-type amino acid, I10(325v), was recognized by the peptide TNSHNY within the CDR1 of Vβ8.3. Therefore, the CDR1 in the Vβ7 or Vβ8.3 might play an important role in recognizing the epitope P18-I10 or I10(325v), respectively, and, in particular, the distance between CDR1 and the amino acid 325V or 325v within the peptide seemed to be essential for recognizing the epitope. Taken together, the results derived from our molecular modeling strategy appear to be consistent with the experimental results.

Although the epitope specificity created by TCRs has been reported to be dependent mainly on the amino acid sequences in the CDR3 regions for both the TCRα and β chains (43,44), crystallographic analyses on various TCR and peptide/MHC interactions have suggested that both the CDR1 and CDR3 in

TABLE 4 The distance between two terminal atoms in the side chain of 325V or 325v and atoms in main chain of the obtained TCR-CDR1 through molecular modeling

Vβ8.3	N(T)	Cα(T)	C(T)	O(T)	N(N)	Cα(N)	C(N)	O(N)	N(S)	Cα(S)	C(S)	O(S)
1hxmBCG1 (325V)	13.34	12.22	11.94	12.32	11.47	11.47	10.62	9.61	11.19	10.74	11.80	12.32
CG2 (325V)	12.54	11.59	11.25	11.41	11.00	10.98	9.90	8.83	10.34	9.64	10.65	11.36
1etzBCG1 (325V)	13.77	13.45	12.19	11.26	12.24	11.31	9.99	8.95	10.16	9.20	9.41	10.25
CG2 (325V)	13.14	12.75	11.63	10.76	11.76	11.02	9.57	8.73	9.41	8.22	8.32	9.30
1fo0ACG1 (325V)	10.43	9.82	9.37	9.20	9.43	9.34	10.58	11.43	10.85	12.07	13.27	13.89
CG2 (325V)	9.41	8.58	8.29	8.45	8.18	8.25	9.66	10.47	10.12	11.47	12.47	13.09
1h5bACG1 (325V)	11.98	10.99	10.34	10.13	10.23	9.81	10.97	12.02	10.95	12.14	12.24	11.29
CG2 (325V)	11.18	10.43	9.87	9.95	9.52	9.16	10.18	11.13	10.20	11.29	11.10	10.02
1dlfLCG1 (325V)	12.46	11.35	10.28	9.72	10.18	9.27	10.19	11.40	9.77	10.82	11.61	11.18
CG2 (325V)	11.39	10.46	9.42	9.14	9.06	8.14	9.06	10.25	8.69	9.75	10.28	9.64
1hxmBCG1 (325v)	11.19	10.04	9.53	9.84	8.98	8.81	7.89	6.96	8.39	7.95	9.00	9.47
CG2 (325v)	10.21	9.16	8.72	8.95	8.37	8.32	7.31	6.25	7.84	7.33	8.47	9.12
1etzBCG1 (325v)	11.63	11.33	10.01	9.08	10.05	9.08	7.83	6.75	8.15	7.37	7.76	8.53
CG2 (325v)	10.57	10.17	9.00	8.11	9.13	8.38	6.95	6.11	6.87	5.78	6.11	7.09
1fo0ACG1 (325v)	8.55	8.16	7.68	7.31	7.99	7.98	9.10	9.82	9.44	10.57	11.78	12.26
CG2 (325v)	6.96	6.31	6.03	6.03	6.22	6.47	7.78	8.44	8.38	9.66	10.67	11.12
1h5bACG1 (325v)	9.98	8.91	8.17	7.84	8.17	7.74	8.99	10.05	9.05	10.33	10.63	9.80
CG2 (325v)	8.70	7.89	7.22	7.27	6.92	6.57	7.69	8.66	7.83	9.04	9.03	8.07
1dlfLCG1 (325v)	10.66	9.50	8.36	7.65	8.40	7.51	8.42	9.61	8.05	9.15	10.11	9.84
CG2 (325v)	9.11	8.13	6.97	6.57	6.70	5.75	6.71	7.91	6.41	7.59	8.30	7.82

Unit of the distance is Å. The code 1hxmB, 1etzB, 1fo0A, 1h5bA, or 1dlfL represents each template protein to determine the structure of Vβ8.3. CG1 and CG2 are two terminal atoms of side chain in 325V or 325v. The successive three amino acids, Thr, Asn, and Ser, within CDR1 of Vβ8.3 are the nearest portion for CG1 or CG2.

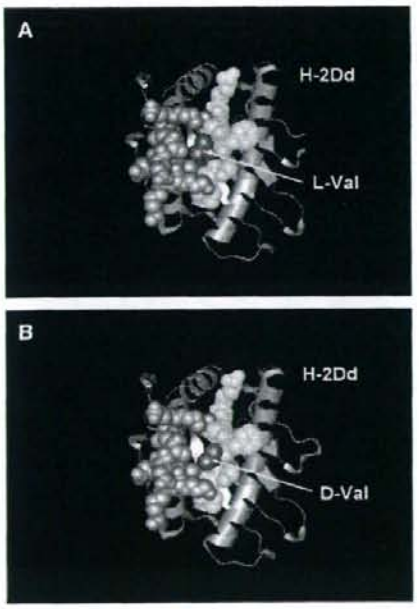

FIGURE 9 (*A* and *B*) 3D structures of P18-I10/H-2D^d complex and I10(325v)/H-2D^d complex. Gray ribbon and ball format represent the H-2D^d class I MHC molecule, and the yellow ball format indicates the D^d-bounded epitope peptide, P18-I10 or I10(325v). In the H-2D^d class I MHC molecule, only the positions for interaction with 325V are drawn in the ball format, for clarity. The L-type of valine (V) and the D-type of valine (v) at position 325 are shown in green and red, respectively. Radius of ball format indicates van der Waals radius.

the TCRα and TCRβ chains might contact with the antigenic peptide/MHC complex (1,2,5,6), particularly with the carboxyl-terminal portion of the peptides (2). Moreover, recent reports have shown that the CDR1 in Vβ10 participated in class I MHC molecule-mediated T-cell recognition (45,46). In these reports, significant alteration in the capacity to bind class I MHC molecules and in the ability to respond to the peptide/MHC complex was demonstrated when a single amino acid substitution was introduced into the CDR1 of TCR Vβ10 by site-directed mutagenesis. Indeed, we have shown here that the CDR1 in the TCRβ chains appeared to interact directly with the key amino acid for determining epitope specificity. Thus, if the most critical amino acid for determining the epitope specificity is located near the C-terminal portion of a peptide such as P18-I10, not only the CDR3 but also the CDR1 in the TCRβ chain may be involved in determining antigen specificity.

It is also important to consider the role of the primary structures in TCR recognition. As demonstrated in Fig. 6 *B*, there are two cysteine (C) residues positioned upstream of CDR1 (*magenta*) and CDR3 (*magenta*) of both TCR Vβ7 and Vβ8.3. These residues bind each other via a disulfide bond and must be a basic structure of TCRs because they are conserved in most of the murine TCR sequences (47) . The two or three amino acids (*blue*) between the conserved cysteine (C) residues and the CDR1 would be key amino acids in forming the 3D structure of CDR1, although they do not interact directly with the epitope peptide. If only these amino acids are exchanged for other amino acids, the 3D structure of CDR1 affecting the recognition of an amino acid at position 325 would change. Indeed, these amino acids are

highly variable for both TCR Vβ7 and Vβ8.3 (Fig. 6 *B*) and for various other murine TCR sequences (47), whereas the regions just after CDR1 are mostly conserved. These amino acids are likely to participate in the peptide recognition by creating small changes in the 3D structure of CDR1. In this regard, both CDR1 and the two or three amino acids between the cysteine (C) and CDR1 may play a important role in recognizing position 325 within P18-I10 or I10(325v).

We thank Dr. Megumi Takahashi for her assistance with the DNA sequence analysis of the TCRs.

This work was supported in part by grants from the Ministry of Education, Science, Sport, and Culture, from the Ministry of Health and Labor and Welfare, Japan; from the Japanese Health Sciences Foundation; and from and by the Promotion and Mutual Aid Corporation for Private Schools of Japan.

REFERENCES

1. Garboczi, D. N., P. Ghosh, U. Utz, Q. R. Fan, W. E. Biddison, and D. C. Wiley. 1996. Structure of the complex between human T-cell receptor, viral peptide and HLA-A2. *Nature*. 384:134–141.
2. Garcia, K. C., M. Degano, R. L. Stanfield, A. Brunmark, M. R. Jackson, P. A. Peterson, L. Teyton, and I. A. Wilson. 1996. An alphabeta T cell receptor structure at 2.5 A and its orientation in the TCR-MHC complex. *Science*. 274:209–219.
3. Garboczi, D. N., and W. E. Biddison. 1999. Shapes of MHC restriction. *Immunity*. 10:1–7.
4. Hennecke, J., and D. C. Wiley. 2001. T cell receptor-MHC interactions up close. *Cell*. 104:1–4.
5. Reiser, J. B., C. Gregoire, C. Darnault, T. Mosser, A. Guimezanes, A. M. Schmitt-Verhulst, J. C. Fontecilla-Camps, G. Mazza, B. Malissen, and D. Housset. 2002. A T cell receptor CDR3beta loop undergoes conformational changes of unprecedented magnitude upon binding to a peptide/MHC class I complex. *Immunity*. 16:345–354.
6. Garcia, K. C., M. Degano, L. R. Pease, M. Huang, P. A. Peterson, L. Teyton, and I. A. Wilson. 1998. Structural basis of plasticity in T cell receptor recognition of a self peptide-MHC antigen. *Science*. 279: 1166–1172.
7. Takahashi, H., J. Cohen, A. Hosmalin, K. B. Cease, R. Houghten, J. L. Cornette, C. DeLisi, B. Moss, R. N. Germain, and J. A. Berzofsky. 1988. An immunodominant epitope of the human immunodeficiency virus envelope glycoprotein gp160 recognized by class I major histocompatibility complex molecule-restricted murine cytotoxic T lymphocytes. *Proc. Natl. Acad. Sci. USA*. 85:3105–3109.
8. Takeshita, T., H. Takahashi, S. Kozlowski, J. D. Ahlers, C. D. Pendleton, R. L. Moore, Y. Nakagawa, K. Yokomuro, B. S. Fox, and D. H. Margulies. 1995. Molecular analysis of the same HIV peptide functionally binding to both a class I and a class II MHC molecule. *J. Immunol.* 154:1973–1986.
9. Takahashi, H., S. Merli, S. D. Putney, R. Houghten, B. Moss, R. N. Germain, and J. A. Berzofsky. 1989. A single amino acid interchange yields reciprocal CTL specificities for HIV-1 gp160. *Science*. 246: 118–121.
10. Takahashi, H., Y. Nakagawa, C. D. Pendleton, R. A. Houghten, K. Yokomuro, R. N. Germain, and J. A. Berzofsky. 1992. Induction of broadly cross-reactive cytotoxic T cells recognizing an HIV-1 envelope determinant. *Science*. 255:333–336.
11. Shirai, M., C. D. Pendleton, and J. A. Berzofsky. 1992. Broad recognition of cytotoxic T cell epitopes from the HIV-1 envelope protein with multiple class I histocompatibility molecules. *J. Immunol.* 148: 1657–1667.
12. Palker, T. J., M. E. Clark, A. J. Langlois, T. J. Matthews, K. J. Weinhold, R. R. Randall, D. P. Bolognesi, and B. F. Haynes. 1988. Type-specific neutralization of the human immunodeficiency virus with antibodies to env-encoded synthetic peptides. *Proc. Natl. Acad. Sci. USA*. 85:1932–1936.
13. Rusche, J. R., K. Javaherian, C. McDanal, J. Petro, D. L. Lynn, R. Grimaila, A. Langlois, R. C. Gallo, L. O. Arthur, P. J. Fischinger, D. P. Bolognesi, S. D. Putney, and T. J. Matthews 1988. Antibodies that inhibit fusion of human immunodeficiency virus-infected cells bind a 24-amino acid sequence of the viral envelope, gp120. *Proc. Natl. Acad. Sci. USA*. 85:3198–3202.
14. Goudsmit, J., C. Debouck, R. H. Meloen, L. Smit, M. Bakker, D. M. Asher, A. V. Wolff, C. J. Gibbs, Jr., and D. C. Gajdusek. 1988. Human immunodeficiency virus type 1 neutralization epitope with conserved architecture elicits early type-specific antibodies in experimentally infected chimpanzees. *Proc. Natl. Acad. Sci. USA*. 85:4478–4482.
15. Takahashi, H., R. N. Germain, B. Moss, and J. A. Berzofsky. 1990. An immunodominant class I-restricted cytotoxic T lymphocyte determinant of human immunodeficiency virus type 1 induces CD4 class II-restricted help for itself. *J. Exp. Med.* 171:571–576.
16. Clerici, M., D. R. Lucey, R. A. Zajac, R. N. Boswell, H. M. Gebel, H. Takahashi, J. A. Berzofsky, and G. M. Shearer. 1991. Detection of cytotoxic T lymphocytes specific for synthetic peptides of gp160 in HIV-seropositive individuals. *J. Immunol.* 146:2214–2219.
17. Takahashi, H., R. Houghten, S. D. Putney, D. H. Margulies, B. Moss, R. N. Germain, and J. A. Berzofsky. 1989. Structural requirements for class I MHC molecule-mediated antigen presentation and cytotoxic T cell recognition of an immunodominant determinant of the human immunodeficiency virus envelope protein. *J. Exp. Med.* 170:2023–2035.
18. Corr, M., L. F. Boyd, E. A. Padlan, and D. H. Margulies. 1993. H-2Dd exploits a four residue peptide binding motif. *J. Exp. Med.* 178:1877–1892.
19. Jorgensen, J. L., U. Esser, B. Fazekas de St Groth, P. A. Reay, and M. M. Davis. 1992. Mapping T-cell receptor-peptide contacts by variant peptide immunization of single-chain transgenics. *Nature*. 355:224–230.
20. Cease, K. B., H. Margalit, J. L. Cornette, S. D. Putney, W. G. Robey, C. Ouyang, H. Z. Streicher, P. J. Fischinger, R. C. Gallo, C. DeLisi, and J. A. Berzofsky. 1987. Helper T-cell antigenic site identification in the acquired immunodeficiency syndrome virus gp120 envelope protein and induction of immunity in mice to the native protein using a 16-residue synthetic peptide. *Proc. Natl. Acad. Sci. USA*. 84:4249–4253.
21. Boehncke, W. H., T. Takeshita, C. D. Pendleton, R. A. Houghten, S. Sadegh-Nasseri, L. Racioppi, J. A. Berzofsky, and R. N. Germain. 1993. The importance of dominant negative effects of amino acid side chain substitution in peptide-MHC molecule interactions and T cell recognition. *J. Immunol.* 150:331–341.
22. Zhang, W., S. Honda, F. Wang, T. P. DiLorenzo, A. M. Kalergis, D. A. Ostrov, and S. G. Nathenson. 2001. Immunobiological analysis of TCR single-chain transgenic mice reveals new possibilities for interaction between CDR3alpha and an antigenic peptide bound to MHC class I. *J. Immunol.* 167:4396–4404.
23. Takahashi, H., Y. Nakagawa, K. Yokomuro, and J. A. Berzofsky. 1993. Induction of $CD8^+$ cytotoxic T lymphocytes by immunization with syngeneic irradiated HIV-1 envelope derived peptide-pulsed dendritic cells. *Int. Immunol.* 5:849–857.
24. Takahashi, H., Y. Nakagawa, G. R. Leggatt, Y. Ishida, T. Saito, K. Yokomuro, and J. A. Berzofsky. 1996. Inactivation of human immunodeficiency virus (HIV)-1 envelope-specific $CD8^+$ cytotoxic T lymphocytes by free antigenic peptide: a self-veto mechanism? *J. Exp. Med.* 183:879–889.
25. Margulies, D. H., G. A. Evans, K. Ozato, R. D. Camerini-Otero, K. Tanaka, E. Appella, and J. G. Seidman. 1983. Expression of H-2Dd and H-2Ld mouse major histocompatibility antigen genes in L cells after DNA-mediated gene transfer. *J. Immunol.* 130:463–470.
26. Abastado, J.P., C. Jaulin, M.P. Schutze, P. Langlade_Demoyen, F. Plata, K. Ozato, and P. Kourilsky. 1987. Fine mapping of epitopes by intradomain K^d/D^d recombinants. *J. Exp. Med.* 166:327–340.
27. Takahashi, M., E. Osono, Y. Nakagawa, J. Wang, J. A. Berzofsky, D. H. Margulies, and H. Takahashi. 2002. Rapid induction of apoptosis in $CD8^+$ HIV-1 envelope-specific murine CTLs by short exposure to antigenic peptide. *J. Immunol.* 169:6588–6593.

28. Bowie, J. U., N. D. Clarke, C. O. Pabo, and R. T. Sauer. 1990. Identification of protein folds: matching hydrophobicity patterns of sequence sets with solvent accessibility patterns of known structures. *Proteins*. 7:257–264.

29. Ota, M., and K. Nishikawa. 1997. Assessment of pseudo-energy potentials by the best-five test: a new use of the three-dimensional profiles of proteins. *Protein Eng.* 10:339–351.

30. Sali, A., and T. L. Blundell. 1993. Comparative protein modelling by satisfaction of spatial restraints. *J. Mol. Biol.* 234:779–815.

31. Fiser, A., R. K. Do, and A. Sali. 2000. Modeling of loops in protein structures. *Protein Sci.* 9:1753–1773.

32. Baker, D., and A. Sali. 2001. Protein structure prediction and structural genomics. *Science*. 294:93–96.

33. Marti-Renom, M. A., M. S. Madhusudhan, A. Fiser, B. Rost, and A. Sali. 2002. Reliability of assessment of protein structure prediction methods. *Structure*. 10:435–440.

34. Achour, A., K. Persson, R. A. Harris, J. Sundback, C. L. Sentman, Y. Lindqvist, G. Schneider, and K. Karre. 1998. The crystal structure of H-2Dd MHC class I complexed with the HIV-1-derived peptide P18–I10 at 2.4 A resolution: implications for T cell and NK cell recognition. *Immunity*. 9:199–208.

35. Stewart, J. J. P. 1996. Application of localized molecular orbitales to the solution of semiempirical self-consistent field equations. *Int. J. Quant. Chem.* 58:133–146.

36. Sherman, D. H., P. S. Hochman, R. Dick, R. Tizard, K. L. Ramachandran, R. A. Flavell, and B. T. Huber. 1987. Molecular analysis of antigen recognition by insulin-specific T-cell hybridomas from B6 wild-type and bm12 mutant mice. *Mol. Cell. Biol.* 7:1865–1872.

37. Tan, K. N., B. M. Datlof, J. A. Gilmore, A. C. Kronman, J. H. Lee, A. M. Maxam, and A. Rao. 1988. The T cell receptor V alpha 3 gene segment is associated with reactivity to *p*-azobenzenearsonate. *Cell*. 54:247–261.

38. Bill, J., J. Yague, V. B. Appel, J. White, G. Horn, H. A. Erlich, and E. Palmer. 1989. Molecular genetic analysis of 178 I-Abm12-reactive T cells. *J. Exp. Med.* 169:115–133.

39. Cerasoli, D. M., M. P. Riley, F. F. Shih, and A. J. Caton. 1995. Genetic basis for T cell recognition of a major histocompatibility complex class II-restricted neo-self peptide. *J. Exp. Med.* 182:1327–1336.

40. Horwitz, M. S., Y. Yanagi, and M. B. Oldstone. 1994. T-cell receptors from virus-specific cytotoxic T lymphocytes recognizing a single immunodominant nine-amino-acid viral epitope show marked diversity. *J. Virol.* 68:352–357.

41. Plaksin, D., K. Polakova, P. McPhie, and D. H. Margulies. 1997. A three-domain T cell receptor is biologically active and specifically stains cell surface MHC/peptide complexes. *J. Immunol.* 158:2218–2227.

42. Bowie, J. U., R. Luthy, and D. Eisenberg. 1991. A method to identify protein sequences that fold into a known three-dimensional structure. *Science*. 253:164–170.

43. Kaye, J., and S. M. Hedrick. 1988. Analysis of specificity for antigen, Mls, and allogenic MHC by transfer of T-cell receptor alpha- and beta-chain genes. *Nature*. 336:580–583.

44. Lai, M. Z., Y. J. Jang, L. K. Chen, and M. L. Gefter. 1990. Restricted V-(D)-J junctional regions in the T cell response to lambda-repressor. Identification of residues critical for antigen recognition. *J. Immunol.* 144:4851–4856.

45. Bellio, M., Y. C. Lone, O. de la Calle-Martin, B. Malissen, J. P. Abastado, and P. Kourilsky. 1994. The V beta complementarity determining region 1 of a major histocompatibility complex (MHC) class I-restricted T cell receptor is involved in the recognition of peptide/MHC I and superantigen/MHC II complex. *J. Exp. Med.* 179: 1087–1097.

46. Lone, Y. C., M. Bellio, A. Prochnicka-Chalufour, D. M. Ojcius, N. Boissel, T. H. Ottenhoff, R. D. Klausner, J. P. Abastado, and P. Kourilsky. 1994. Role of the CDR1 region of the TCR beta chain in the binding to purified MHC-peptide complex. *Int. Immunol.* 6: 1561–1565.

47. Clark, S. P., B. Arden, D. Kabelitz, and T. W. Mak. 1995. Comparison of human and mouse T-cell receptor variable gene segment subfamilies. *Immunogenetics*. 42:531–540.

Selective Transmission of R5 HIV-1 over X4 HIV-1 at the Dendritic Cell–T Cell Infectious Synapse Is Determined by the T Cell Activation State

Takuya Yamamoto[1,2☯], Yasuko Tsunetsugu-Yokota[1☯*], Yu-ya Mitsuki[1,3], Fuminori Mizukoshi[1], Takatsugu Tsuchiya[1], Kazutaka Terahara[1], Yoshio Inagaki[3], Naoki Yamamoto[4], Kazuo Kobayashi[1], Jun-ichiro Inoue[4]

1 Department of Immunology, National Institute of Infectious Diseases, Shinjuku-ku, Tokyo, Japan, 2 Division of Cellular and Molecular Biology, Department of Cancer Biology, Institute of Medical Science, University of Tokyo, Minato-ku, Tokyo, Japan, 3 Department of Molecular Virology, Bio-Response, Tokyo Medical and Dental University, Bunkyo-ku, Tokyo, Japan, 4 AIDS Research Center, National Institute of Infectious Diseases, Shinjuku-ku, Tokyo, Japan

Abstract

Dendritic cells (DCs) are essential antigen-presenting cells for the induction of T cell immunity against HIV. On the other hand, due to the susceptibility of DCs to HIV infection, virus replication is strongly enhanced in DC–T cell interaction via an immunological synapse formed during the antigen presentation process. When HIV-1 is isolated from individuals newly infected with the mixture of R5 and X4 variants, R5 is predominant, irrespective of the route of infection. Because the early massive HIV-1 replication occurs in activated T cells and such T-cell activation is induced by antigen presentation, we postulated that the selective expansion of R5 may largely occur at the level of DC–T cell interaction. Thus, the immunological synapse serves as an infectious synapse through which the virus can be disseminated *in vivo*. We used fluorescent recombinant X4 and R5 HIV-1 consisting of a common HIV-1 genome structure with distinct envelopes, which allowed us to discriminate the HIV-1 transmitted from DCs infected with the two virus mixtures to antigen-specific $CD4^+$ T cells by flow cytometry. We clearly show that the selective expansion of R5 over X4 HIV-1 did occur, which was determined at an early entry step by the activation status of the $CD4^+$ T cells receiving virus from DCs, but not by virus entry efficiency or productivity in DCs. Our results imply a promising strategy for the efficient control of HIV infection.

Citation: Yamamoto T, Tsunetsugu-Yokota Y, Mitsuki Y-y, Mizukoshi F, Tsuchiya T, et al. (2009) Selective Transmission of R5 HIV-1 over X4 HIV-1 at the Dendritic Cell–T Cell Infectious Synapse Is Determined by the T Cell Activation State. PLoS Pathog 5(1): e1000279. doi:10.1371/journal.ppat.1000279

Editor: Michael Farzan, Harvard Medical School, United States of America

Received August 14, 2008; **Accepted** December 23, 2008; **Published** January 30, 2009

Funding: This work was supported by a grant for Research on HIV/AIDS from the Ministry of Health, Labour and Welfare of Japan. FM received support from the Japanese Foundation for AIDS Prevention. TY was supported by Research Fellowships of the Japan Society for the promotion of Science for Young Scientists.

Competing Interests: The authors have declared that no competing interests exist.

* E-mail: yyokota@nih.go.jp

☯ These authors contributed equally to this work.

Introduction

HIV-1 infects T cells and monocyte lineage cells, including macrophages and dendritic cells (DCs), through CD4, the primary receptor for entry. The cellular tropism of HIV-1, i.e., macrophage (M)-tropic or T-cell line (T)-tropic, is determined by chemokine receptors. Depending on whether they mainly use the CCR5 or CXCR4 entry coreceptors, primary isolates are defined as R5 for M-tropic and X4 for T-tropic variants, respectively [1]. Despite the fact that the HIV-1 present in infected individuals frequently comprises the mixture of R5 and X4, virus isolated from individuals newly infected through sexual, parenteral, or mother-to-child transmission is also predominantly R5 [2,3,4]. During the clinical course of disease progression, the phenotype of the virus may evolve from R5 to X4 or to R5/X4-dual tropic [5,6,7], and X4 virus has been shown to be associated with a decline in $CD4^+$ T cell counts and the onset of clinical symptoms of AIDS [8]. However, R5 and X4 viruses are equally cytopathic [9], and R5 virus isolated from patients with late-stage disease are similarly pathogenic to X4 *in vitro* [10]. These findings suggest that an yet-unknown selective mechanism that favors R5 virus exists during transmission and/or the early phases of infection in the host (review in [11]).

DCs are important antigen-presenting cells that initiate an immune response by activating naïve and memory $CD4^+$ T cells [12]. Although it is known that DCs are susceptible to HIV-1 infection, virus productivity from DCs and R5/X4 preferences for DCs vary (see review in [13]). This could be attributed in large part to the heterogeneous nature of DC sources, maturation levels, proliferative capacities, methods for isolation, and culture conditions. Importantly, all DC subsets express CD4 and varying levels of CXCR4 and CCR5.

Because of the low frequency of DCs *in vivo*, blood monocytes are often utilized as representative myeloid DCs for the study of HIV-1 infection. We showed earlier that although monocyte-derived DCs (MDDCs) generated *in vitro* are susceptible to X4 and R5 HIV-1 infection, R5-infected DCs are poorly productive compared with R5-infected macrophages of the same monocyte origin [14]. Nevertheless, HIV-infected MDDCs efficiently transmit virus to autologous $CD4^+$ T cells [15,16,17], by close contact between MDDCs and $CD4^+$ T cells. Thus, when HIV-infected DCs present antigens to $CD4^+$ T cells in lymphoid organs,

Author Summary

The cellular tropism of HIV-1 is determined by the binding of HIV-1 envelope to chemokine coreceptors, CCR5 or CXCR4, in addition to a major entry receptor, CD4. The mystery still now is that despite the mixed infection of CCR5-utilizing (R5) and CXCR4-utilizing (X4) HIV-1 in many AIDS patients, R5 is predominantly isolated from newly infected individuals whatever the mode of infection. Because the early massive HIV-1 replication occurs in activated T cells and such T-cell activation is induced initially by antigen-presenting DCs, we postulated that the selective expansion of R5 may largely occur at the level of antigen-dependent DC–T cell interaction, called immunological synapse. Thus, the immunological synapse serves as an infectious synapse through which the virus can be rapidly disseminated *in vivo*. In this study, we prepared X4 and R5 HIV-1 expressing red or green fluorescence and showed that the selective expansion of R5 over X4 did occur, depending on the activation status of $CD4^+$ T cells receiving virus from DCs, but not by virus entry efficiency or productivity in DCs.

an immunological synapse is formed and a T cell–activation program proceeds, which allows virus transmitted from DCs to replicate in activated $CD4^+$ T cells. This interaction is called an infectious synapse [18,19]. Thus, efficient HIV transmission from DCs to $CD4^+$ T cells through infectious synapses may play a central role not only for the massive expansion of HIV following initial infection, but also for generating latent infection in HIV-specific memory $CD4^+$ T cells [13].

The expression level of CXCR4 does not appear to be a crucial factor of X4 replication, because most circulating hematopoietic cells, including $CD4^+$ T cells and DCs [20], or submucosal lymphocytes [21] express CXCR4 albeit at various levels. Although the abundant CCR5 expression in activated/memory $CD4^+$ T cells in submucosa may explain the preferential sexual transmission of R5 HIV-1, there are many more $CXCR4^+$ $CD4^+$ T cells than there are $CCR5^+$ $CD4^+$ T cells in the blood [11,22]. Furthermore, MDDCs, and macrophages from the same individual express similarly low levels of CCR5 [23] despite large differences in R5 virus productivity. Cavrois et al. recently analyzed the fusion activity of labeled virion with DC membranes and showed that the fusion efficiency of R5 declined as DCs matured and CCR5 expression decreased, and that X4 fusion efficiency did not change with maturation [24]. On the other hand, Pion et al. showed that fusion of X4 with immature DCs was markedly inefficient compared with that of R5, and that this inefficiency was not complemented by ectopic expression of CXCR4 [25]. They hypothesized that an as-yet unknown env-specific block early in the virus infection cycle occurs in DCs, which is not due solely to surface expression level of chemokine receptors.

The state of T-cell activation determines the level of HIV-1 replication. HIV-1 replication in resting primary $CD4^+$ T cells is inefficient at every level after entry: reverse transcription, nuclear import, integration, and transcription [26,27]. Interestingly, a significant replicative advantage of R5 over X4 HIV-1 in some $CD4^+$ T cell clones is reported and X4-dependent restriction of HIV replication is rescued by T cell receptor (TcR) stimulation [28]. In TcR-stimulated $CD4^+$ T cells, R5, but not X4, HIV-1 efficiently replicates in the absence of MEK/ERK signaling, whereas nuclear import of X4 HIV-1 is dependent on the MEK/ERK pathway [29]. Recently, Cicala et al. showed that R5 ENV up-regulates the expression of genes belonging to MAP kinase pathways and genes regulating the cell cycle to a greater extent than X4 ENV [30]. Stronger modulation of transcription by R5 than by X4 viruses in $CD4^+$ T cells was also reported [31]. These results suggest that R5 HIV-1 has an advantage in establishing the infection cycle in $CD4^+$ T cells. The question is how this mechanism contributes to the selective expansion of R5 virus early in HIV-1 infection.

To study the preference of R5 or X4 HIV-1 transmission during DC-T cell interaction, we produced highly replication-competent, fluorescent viruses of X4 and R5 type. We analyzed the HIV-1 life cycle in MDDCs and $CD4^+$ T cells, before and after coculture, by quantitative PCR (qPCR) and FACS. Although the infection process progressed at an equal rate in MDDCs infected with either R5 or X4 virus, R5 virus predominantly replicated in $CD4^+$ T cells which are activated by antigen-presenting HIV-infected MDDCs.

Results

HIV-1 expressing EGFP or DsRed is replication competent in PHA-activated PBMCs

We generated fluorescent X4 (HIV-$1_{NL\text{-}D}$) and R5 (HIV-$1_{NLAD8\text{-}D}$) viruses. The structure of these provirus clones and HIV-$1_{NL\text{-}E}$ [32] was depicted in Fig. 1A. The co-receptor usage of these viruses was determined by 1G5 or 1G5/CCR5 cells, which contain a LTR-driven luciferase gene [33]. As shown in Fig. 1B, both 1G5 and 1G5/CCR5 are infected with X4 type virus (HIV-$1_{NL\text{-}E}$ and HIV-$1_{NL\text{-}D}$), whereas 1G5/CCR5, but not 1G5, is infected with R5 HIV-1 (HIV-$1_{NLAD8\text{-}D}$), indicating the expected coreceptor usage.

By combining X4 HIV-$1_{NL\text{-}E}$ and R5 HIV-$1_{NLAD8\text{-}D}$, it became easy to monitor their replication in individual cells using FACS. These viruses were prepared by transfecting proviral DNA into 293T cells. We infected PBMCs stimulated with phytohemagglutinin (PHA blasts) from two donors with the same p24 Gag amount of the prototype virus HIV-1_{NL432} or with fluorescent viruses HIV-$1_{NL\text{-}E}$, HIV-$1_{NL\text{-}D}$, or HIV-$1_{NLAD8\text{-}D}$ and then monitored the kinetics of HIV-1 replication (Fig. 2A). Because *nef* is not deleted in these constructs, the infectivity of the fluorescent viruses is preserved and comparable to that of wild-type virus. When cells were analyzed by FACS at 7 d post-infection (dpi), we were able to clearly detect EGFP- or DsRed-positive $CD3^+$ T cell populations (Fig. 2B). Therefore, these fluorescent viruses are useful tools with which to identify HIV-infected cell populations.

HIV-1 transmitted from infected MDDCs to $CD4^+$ T cells during antigen presentation is predominantly the R5 variant

Next, we determined which HIV-1 variant preferentially replicates in $CD4^+$ T cells that have been activated by interacting with HIV-infected immature MDDCs. We mixed an equal amount of p24-measured HIV-$1_{NL\text{-}E}$ and HIV-$1_{NLAD8\text{-}D}$, and infected MDDCs. We then cocultured the infected MDDCs with allogeneic $CD4^+$ T cells. As shown in Fig. 3A, HIV-1 replication was detectable at 7 dpi in the culture supernatant of the MDDC–T cell coculture of DCs (DC-1 or DC-2) and $CD4^+$ T cells (allo T-3 or allo T-4). As reported previously, MDDCs themselves produce little if any virus during cultivation [14], and we were unable to detect $EGFP^+$ or $DsRed^+$ MDDCs at 7 dpi (data not shown). When day 3 PHA blasts were directly infected with the virus mixture, cells infected with X4 viruses expressing EGFP (HIV-$1_{NL\text{-}E}$) predominated at 7 dpi (Fig. 3B). This may be due to the reduced expression of CCR5 in day 3 PHA blasts [22]. In contrast, in most of the combinations of MDDCs and allogeneic

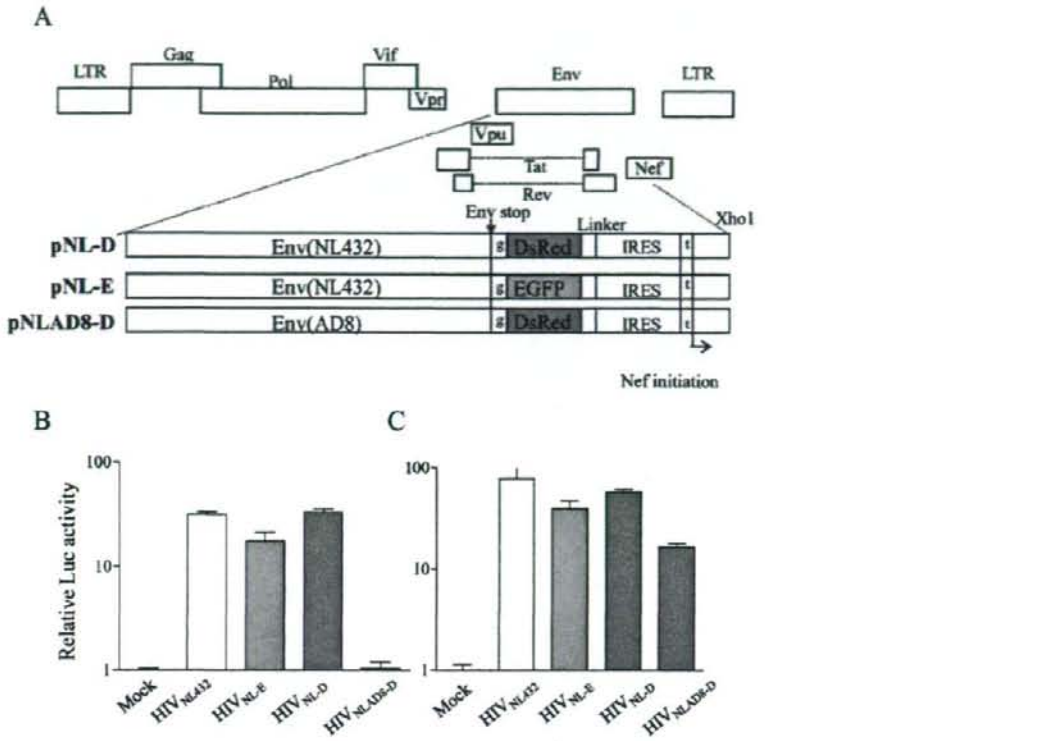

Figure 1. Genomic structure and co-receptor usage of recombinant HIV-1 encoding EGFP or DsRed. (A) The structure of provirus DNA encoding *EGFP* or *DsRed* designated as pNL-E and pNL-D for X4 HIV-1 and pNLAD8-D for R5 HIV-1. EGFP or DsRed is not expressed as a fusion protein of Env because of one base insertion after the Env stop codon. Nef is also independently expressed under the control of IRES. To confirm the coreceptor usage of these fluorescent HIV-1, 1G5 (B) cells, 1G5/CCR5 (C) cells were infected with HIV-1_{NL432} (parent strain), HIV-1_{NL-E}, HIV-1_{NL-D}, or HIV-$1_{NLAD8-D}$. After 48 h post-infection, cell lysates were prepared and the Luc assay was performed. The data represents the averages ±SD of three independent experiments.
doi:10.1371/journal.ppat.1000279.g001

$CD4^+$ T cells (more than 10), cells infected with R5 virus expressing DsRed (HIV-$1_{NLAD8-D}$) were the predominant population, producing virus at 10 dpi (Fig. 3C). The representative results of two MDDC donors (DC-1 and DC-2) cocultured with allogeneic T cells from two donors (T-3 and T-4) were shown here. Of note, a substantial replication of X4 virus was detected only in DC-1/allo T-3 combination, indicating that the activation of this donor's $CD4^+$ T cells (T-3) by allogeneic DC (donor-1) is exceptionally powerful.

We also examined the replicability of R5 and X4 virus under physiological conditions in which DC–T cell interactions occur during antigen-specific immune responses. As shown in Fig. 3D, R5 virus replicated predominantly in PPD- and CMV-reactive $CD4^+$ T cells at 9 dpi (middle and right). In PHA- stimulated T cells, however, both R5 and X4 virus were able to replicate at 7 dpi (left), which is quite similar situation to DC-1/allo T-3 combination (Fig. 3C). We obtained consistent results with cells from several donors during both allogeneic and antigen-specific interactions between MDDCs and $CD4^+$ T cells. Our results suggest that R5 virus has an advantage over X4 virus during transmission from MDDCs to $CD4^+$ T cells.

Similar Infectivity of X4 and R5 HIV-1 in MDDCs

There is some controversy regarding the difference between X4 and R5 virus susceptibility among DC subsets. Some reports indicate that immature MDDCs are more susceptible to R5 virus than to X4 [16,34,35], which may partly explain predominant R5 transmission. Therefore, we felt that it was necessary to determine the efficiency of infection of X4 and R5 in MDDCs. First, we checked the level of coreceptor expression in immature MDDCs. The representative results of several individuals are shown in Fig. 4A. The lower expression level of CCR5 compared with CXCR4 (Fig. 3A) in immature MDDCs is quite consistent with the pattern reported by Cavrois et al. [24], who utilized exactly the same protocol for MDDC preparation.

To analyze early steps after HIV-1 entry, we infected MDDCs with the same p24-measured amount of either HIV-1_{NL-E} or HIV-$1_{NLAD8-D}$ and prepared cell lysates at 8 h post-infection (hpi). We measured the amount of distinct forms of proviral DNA (*R-U5* and *U5-gag*) by qPCR as previously described [36]. The amount of these DNA forms was normalized to that of β-globin. Unfortunately, the copy number of *R-U5*, the earliest reverse transcription product in MDDCs, was too low and varied too much among

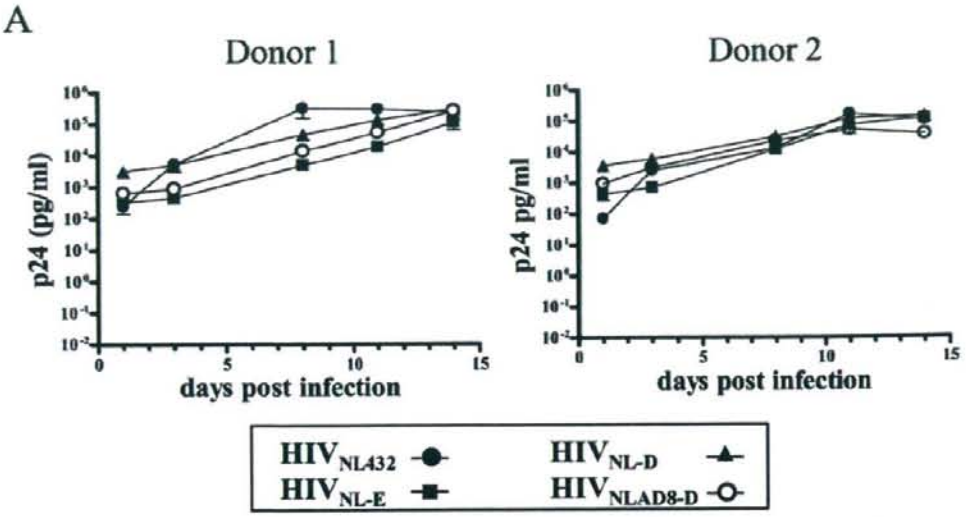
A
Donor 1
Donor 2
p24 (pg/ml)
p24 pg/ml
days post infection
days post infection
HIV NL432
HIV NL-E
HIV NL-D
HIV NLAD8-D

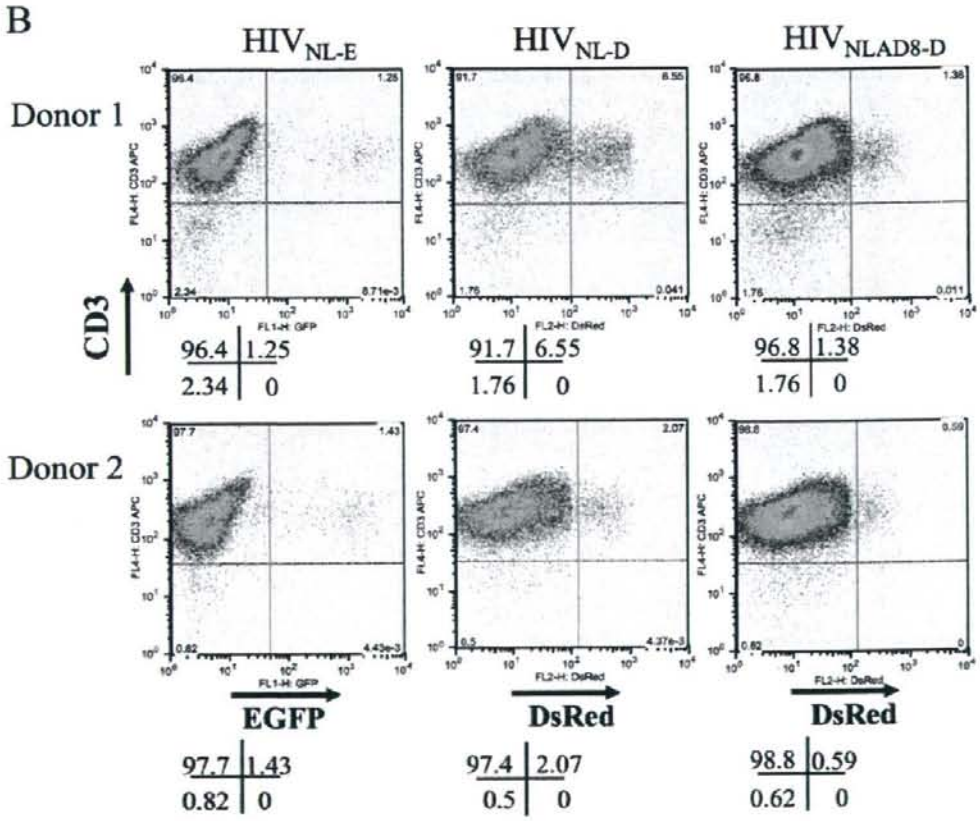
B
HIV NL-E
HIV NL-D
HIV NLAD8-D
Donor 1
Donor 2
CD3
EGFP
DsRed
DsRed
96.4 1.25
2.34 0
91.7 6.55
1.76 0
96.8 1.38
1.76 0
97.7 1.43
0.82 0
97.4 2.07
0.5 0
98.8 0.59
0.62 0

Figure 2. Replication of recombinant HIV-1 encoding EGFP or DsRed. (A) Concentration of X4 HIV-1 (HIV_{NL-432}), X4 HIV-1 expressing EGFP (HIV_{NL-E}), X4 HIV-1 expressing DsRed (HIV_{NL-D}), or R5HIV-1 expressing DsRed ($HIV_{NLADB-D}$) in PHA-stimulated PBMCs of two donors. Virus production was monitored by in-house p24 antigen ELISA. (B) FACS analysis of HIV-1-infected T cells expressing EGFP or DsRed at 7 dpi.
doi:10.1371/journal.ppat.1000279.g002

individuals to allow us to evaluate the differences in entry step of X4 and R5. However, similar amounts of the late reverse transcription product *U5-gag* were consistently detected in X4- or R5-infected MDDCs. A representative result is shown in Fig. 4B. We also tested the infectivity of these viruses in MDDCs by utilizing HIV-1 in which the gene encoding *Renilla* luciferase

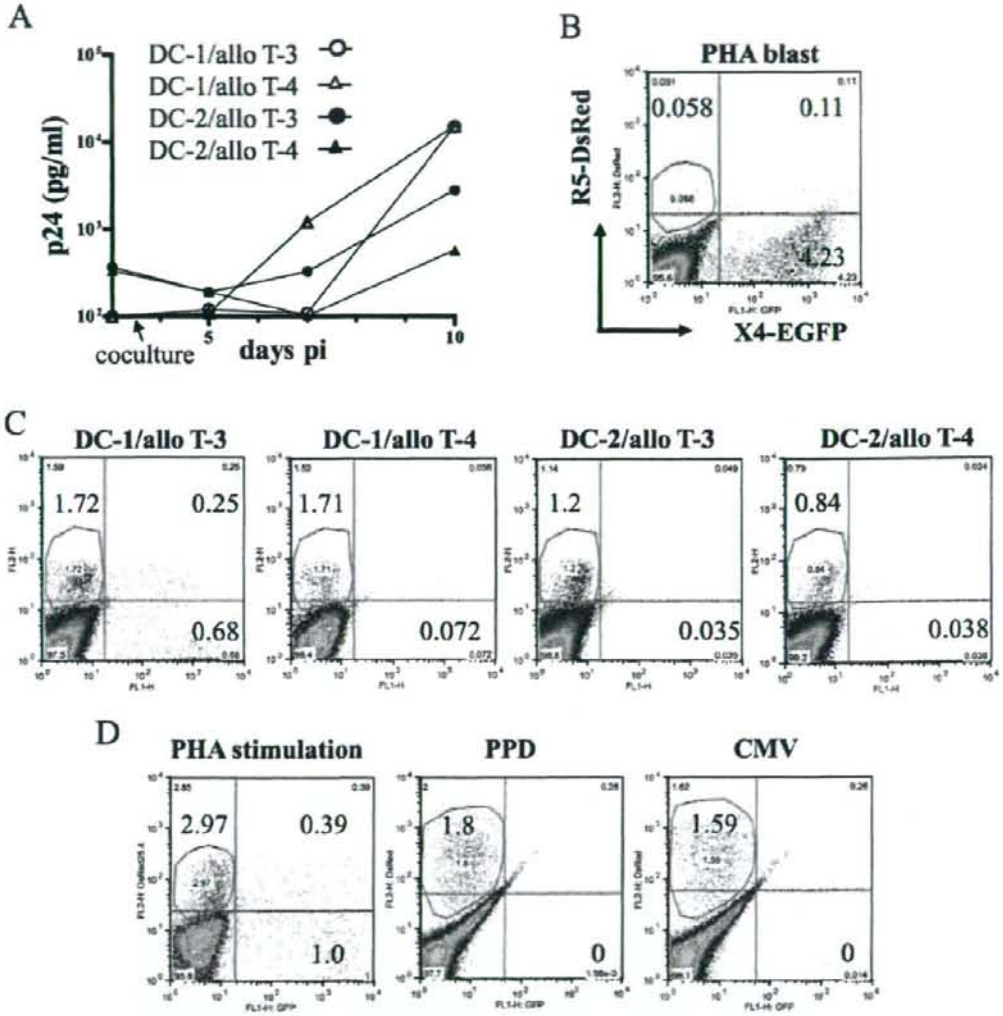

Figure 3. Transmission of HIV-1 from infected MDDCs to $CD4^+$ T cells. (A) Virus production as measured by in-house p24 antigen ELISA in $CD4^+$ T cells cocultured with MDDCs infected with the same amount of HIV_{NL-E} and $HIV_{NLADB-D}$ Culture supernatants were harvested every 3–4 d. (B) FACS analysis of PHA blast T cells which were directly infected with the mixture of R5 and X4 HIV-1 at 7 dpi. (C) allogeneic $CD4^+$ T cells cocultured with HIV-infected MDDCs at 10 dpi. Live (PI^-) and $CD3^+$ T cells were gated. (D) FACS analysis of autologous $CD4^+$ T cells cocultured with infected MDDCs in the presence of PHA (left), PPD antigen (middle) or CMV-infected cell lysate (right). Live (PI^-) and $CD3^+$ T cells were gated.
doi:10.1371/journal.ppat.1000279.g003

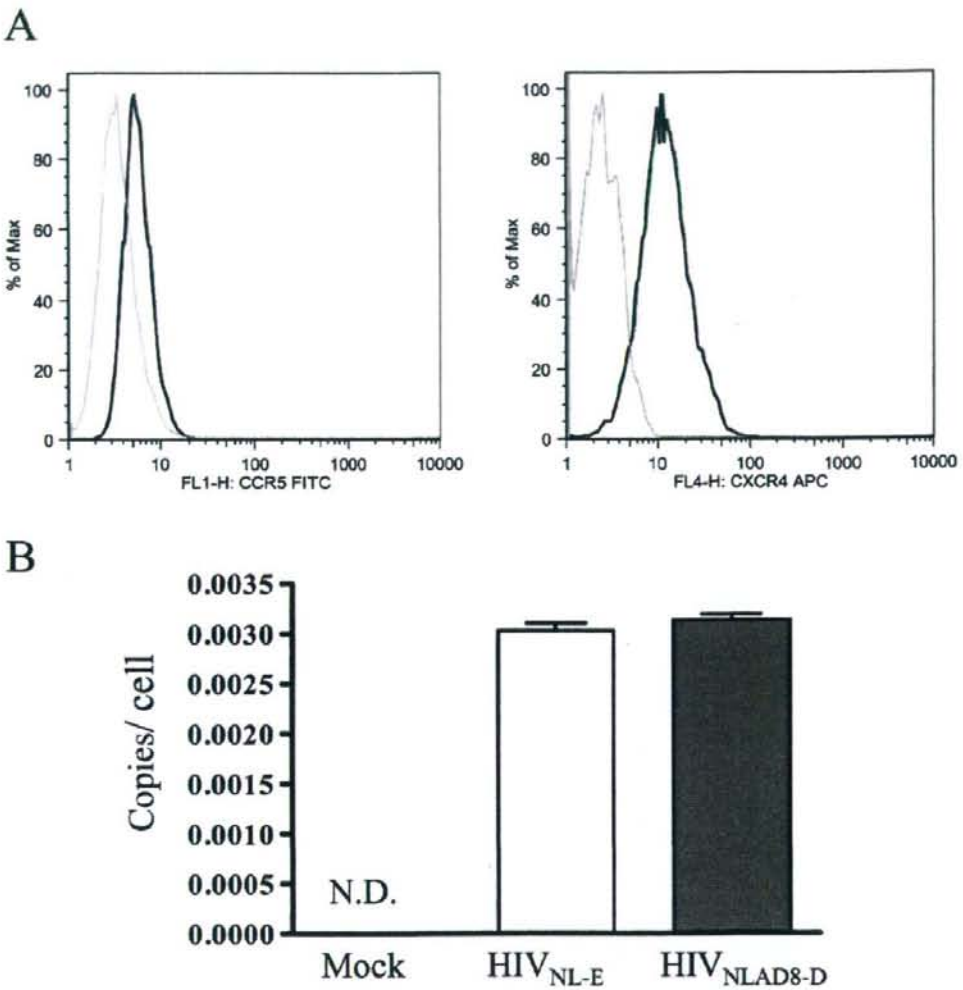

Figure 4. Infectivity of HIV-1 in MDDCs. (A) Surface expression of CCR5 and CXCR4 in MDDCs. MDDCs were stained with anti-CCR5 (left) and anti-CXCR4 mAb (right), or with isotype control mAbs (dotted line). The reproducible representative of the FACS profiles of several individuals is depicted. (B) Quantitative PCR analysis of R5 ($HIV_{NLAD8-D}$) and X4 (HIV_{NL-E}) HIV-1-infected MDDCs. Data represent the average ±SD of three independent experiments.
doi:10.1371/journal.ppat.1000279.g004

(hRluc) is inserted in replacement of DsRed or EGFP gene. The hRluc activities of R5 and X4 viruses did not differ in infected MDDCs at 3 dpi (data not shown). Thus, our results suggest that selective transmission of R5 over X4 HIV-1 from DCs to T cells is not due to differences in early entry, reverse transcription, integration, or transcription in MDDCs.

Selective transmission of R5 over X4 HIV-1 through an infectious synapse depends on the T cell activation state

Suppose R5 and X4 viruses infect MDDCs and are transmitted to $CD4^+$ T cells with similar efficiency, it could be that selective replication of R5 virus in DC–T cell coculture depends on the state of T cell activation. To determine whether this is so, we controlled the activation state of $CD4^+$ T cells by varying TcR-stimulation conditions, and then we analyzed the infectivity of HIV-1_{NL-E} and HIV-$1_{NLAD8-D}$ in these cells (Fig. 5A). Prior to infection with HIV-1, autologous $CD4^+$ T cells were (1) unstimulated, (2) stimulated with 5 μg/ml anti-CD3 and 10 μg/ml anti-CD28 for 24 h (strong activation), (3) stimulated with the same concentrations of anti-CD3 and anti-CD28 for 2 h (medium activation), or (4) stimulated with 10-fold lower concentrations of anti-CD3 and anti-CD28 for 2 h (weak activation). These $CD4^+$ T cells were infected with the virus mixture and analyzed at 5 dpi.

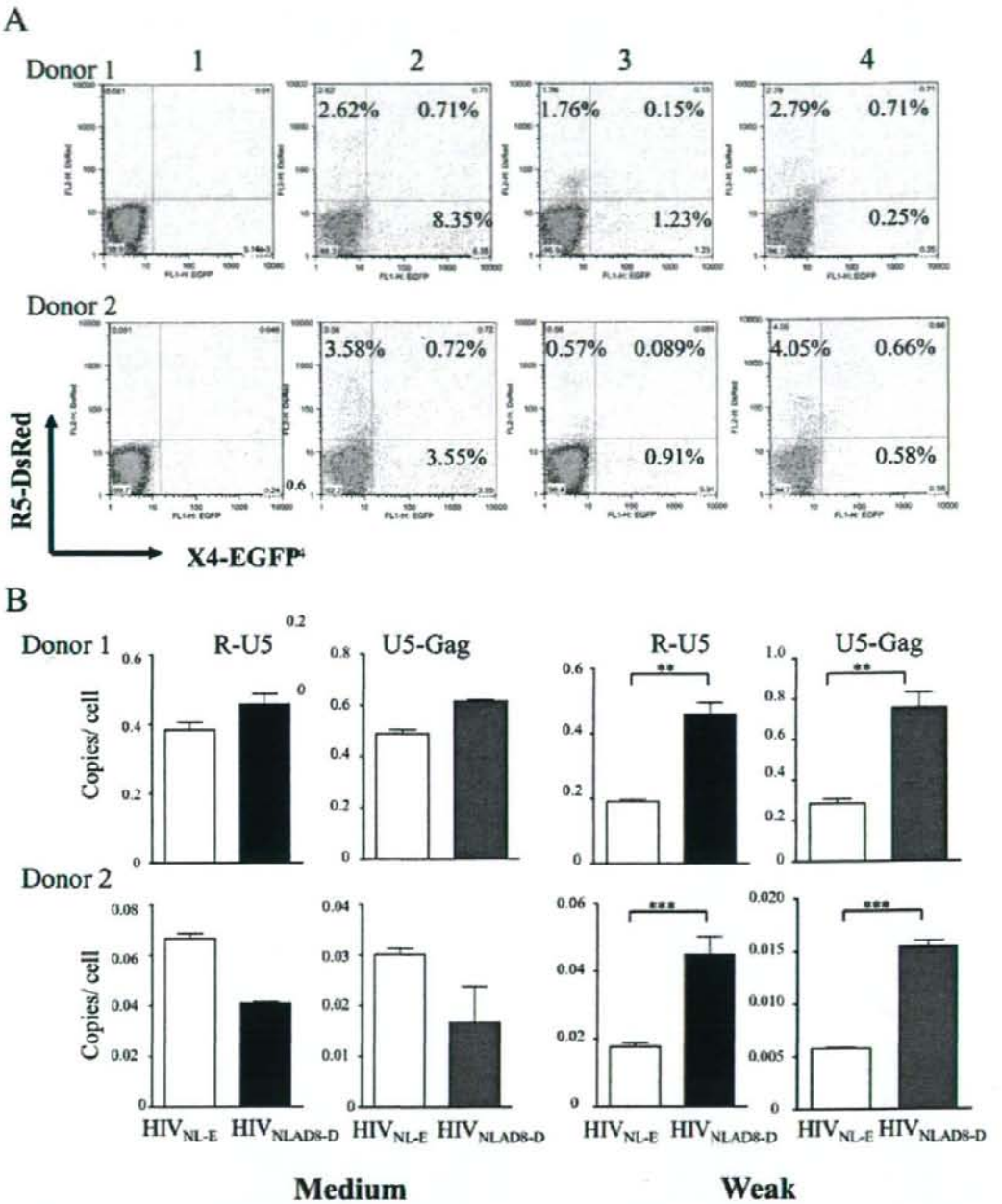

Figure 5. FACS-based analysis of dual infection in primary CD4⁺ T cells. (A) FACS analysis of primary CD4⁺ T cells (1) unstimulated, (2) stimulated with 5 μg/ml anti-CD3 and 10 μg/ml anti-CD28 for 24 h (strong activation), (3) stimulated with the same concentrations of anti-CD3 and anti-CD28 for 2 h (medium activation), or (4) stimulated with 10-fold lower concentrations of anti-CD3 and anti-CD28 for 2 h (weak activation). Cells were then infected with equal amounts of X4 and R5 HIV-1 and analyzed at 5 dpi. (B) Quantitative PCR analysis of CD4⁺T cells separately infected with either R5 or X4 HIV-1. R-U5 and U5-Gag was analyzed by qPCR in two donors. The amount of HIV-1–specific DNA per cell was normalized to β-globin gene expression. The data represents the average ±SD of three independent experiments. **, $P<0.005$; ***, $P<0.0005$.
doi:10.1371/journal.ppat.1000279.g005

Fig. 5 shows the reproducible representative results in cells from two of the six donors. Notably, in the weakly activated $CD4^+$ T cells, only R5 HIV-1 replicated (Fig. 5A-4), whereas both X4 and R5 virus replicated in different cells following medium activation (Fig. 5A-3), and cells that were doubly infected with both X4 and R5 were detected after strong activation condition (Fig. 5A-2). Using the same weak and medium activation conditions, we quantified the early *R-U5* and *U5-gag* forms of HIV-1 reverse transcription products in $CD4^+$ T cells in these donors at 8 hpi. The amount of *R-U5 and U5-gag* DNA did not differ significantly between X4 HIV-1- and R5 HIV-1-infected $CD4^+$ T cells following medium activation (Fig. 5B, left, blank and filled column, respectively). Surprisingly, however, after weak activation, the amount of proviral DNA was dramatically higher in the R5 HIV-1-infected cells compared with those cells infected with X4 (Fig. 5B, right) (**$P<0.005$ and ***$P<0.0005$, in Donor 1 and 2, respectively). These results suggest that the activation state of $CD4^+$ T cells is a key factor in determining selective R5 HIV transmission and virus expansion during DC–T cell interactions.

As shown in Fig. 3, R5 was the HIV-1 variant predominantly transmitted during antigen-specific DC and $CD4^+$ T cell interaction. To determine whether or not the activation state of $CD4^+$ T cells stimulated by antigen-presenting MDDCs is relevant to that of $CD4^+$ T cells weakly TcR stimulated with anti-CD3 and anti-CD28, we first analyzed the expression levels of CCR5 and CXCR4 on $CD4^+$ T cells activated by anti-CD3 and anti-CD28 or MDDCs (Fig. 6). Primary resting $CD4^+$ T cells were cocultured with allogeneic MDDCs (allo) for either 2 or 24 h. Alternatively, primary resting $CD4^+$ T cells were either unstimulated, strong or weak TcR stimulated for 2 h. We did not observe a substantial difference with respect to the surface expression of HIV entry coreceptors 2 h stimulation following any of the conditions. The FACS profile of unstimulated and strongly TcR-stimulated $CD4^+$ T cells is depicted in Fig. 6A. Although these cells were also analyzed for surface activation markers (CD69, CD25, and HLA-DR), no difference was observed. We, therefore, compared the mRNA expression levels of IFN-γ and IL-2, two representative markers of early TcR activation, in these cells by quantitative reverse transcription-PCR (qRT-PCR). The results in cells from two donors are shown in Fig. 6B. The expression level of IFN-γ in allo (oblique lined column) and weak (grey column) stimulation was similar at 2 h and it increased more than 10-fold in strong (black column) stimulation. After 24 h of weak stimulation, IFN-γ increased to a level equivalent to that seen after 2 h strong stimulation (data not shown), but IFN-γ expression in allo-stimulated $CD4^+$ T cells did not reach the maximum level even after 24 h. In both donors, IL-2 mRNA expression was detectable only after strong stimulation for 24 h (data not shown). Thus, both X4 and R5 HIV-1 replicate well in strongly activated $CD4^+$ T cells, but R5 virus is the variant capable of replicating in $CD4^+$ T cells during DC-mediated antigen-specific activation, which may be more closely mimic *in vivo* situation.

Discussion

Why HIV-1 isolated from individuals newly infected with both R5 and X4 variants should be predominantly R5, irrespective of the route of infection, is a longstanding discussion [11]. Because DCs are one of the initial targets for HIV-1 infection and a source of virus dissemination, their role in AIDS pathogenesis has also been the recent topic of much discussion [13,19,37]. HIV-infected DCs, albeit at low productivity, may form infectious synapses with $CD4^+$ T cells during antigen-specific immune response in draining lymph nodes, and efficient HIV-1 transmission and expansion may occur in this microenvironment. The question that we sought to address was whether the predominance of R5 HIV-1 over X4 was determined at the level of DCs or $CD4^+$ T cells and by what mechanism. By analyzing R5 selection during antigen-dependent MDDC–$CD4^+$ T cell HIV-1 transmission, we showed that MDDCs were infected with R5 and X4 HIV-1 and produced low but similar levels of proviral DNAs. We also found that while HIV-1 transmission from MDDCs to $CD4^+$ T cells was predominantly R5, transmission from MDDCs to preactivated $CD4^+$ T cells *in vitro* was slightly more X4 predominant. Although the possibility that this R5 dominancy is ascribed to a unique property of HIV-1_{ADA} envelope is not formally excluded, we showed here that the selective expansion of R5 over X4 *in vivo* may be determined by the activation status of $CD4^+$ T cells, but not by the efficiency of virus entry or productivity in MDDCs. The CCR5 and CXCR4 expression levels appear to contribute little to the predominance of R5 HIV-1 transmission from MDDCs to $CD4^+$ T cells.

DCs are thought to be involved in the sexual transmission of HIV-1 [37]. Rescigno et al. showed that murine submucosal DCs extend their dendrites to the intestinal luminal surface [38], indicating that it may be possible for HIV to directly come into contact with and infect DCs, although how susceptible human submucosal DCs are to X4 and R5 HIV-1 infection is not known. Supporting an alternative infection hypothesis, Bomsel showed that HIV-1 entered through the epithelial barrier and was transmitted to submucosal DCs and $CD4^+$ T cells by transcytosis [39]. Interestingly, Meng et al. reported that human mucosal epithelial cells express CCR5, but not CXCR4. By infecting these cells with equal amounts of R5 and X4 virus, only R5 HIV-1 variant was transmitted, which was determined based on the sequence of the gp120 *env* V3 region [40]. In contrast, Bobardt et al. recently demonstrated that genital epithelia expresses low levels of CCR5 and CXCR4 and that only limited amounts of HIV-1 were transcytosed, without no preference for R5 or X4 [41]. In a monkey model of intravaginal simian immunodeficiency virus (SIV) infection, the infected cells appeared to be DCs in the lamina propria or intraepithelium [42,43]. However, because of the low productivity HIV-1 in DCs, it will be quite difficult to clarify the role of submucosal DCs during early HIV-1 infection in humans. What is most important, however, is not the level of HIV-1 productivity in infected submucosal DCs, but the migratory nature of these DCs to regional lymph nodes.

Resting primary $CD4^+$ T cells are refractory to viral replication; the magnitude of viral replication in these cells is closely linked to their activation state [44]. The R5 HIV-1 envelope protein is known to deliver a signal that activates T cells to some extent [30], which may assist R5 HIV-1 following cell entry to accomplish reverse transcription, nuclear transport, and integration. The lack of such a signal through CXCR4 may explain why X4 virus is more strongly restricted than is R5 virus in primary $CD4^+$ T cells [29]. In fact, we showed that weak activation conditions support R5 HIV-1 replication, whereas stronger activation conditions support replication of both viruses equally well (Fig. 4). When MDDCs interacted with alloantigen- or nominal antigen-specific $CD4^+$ T cells through an immunological synapse, T cells received a signal from TcR first, followed by secondary signals from costimulatory adhesion molecules, resulting in early cytokine production. The intracellular environment of activated T cells under these conditions may be akin to the weak activation of T cells by TcR. The expression level of IFN-γ 2 h after T cell activation by alloantigen or by weak TcR stimulation was similarly low compared to that by strong TcR stimulation (Fig. 6B). We conclude from these results that the initial T-cell activation occurs weakly during DC–$CD4^+$ T cell interactions, and that this low

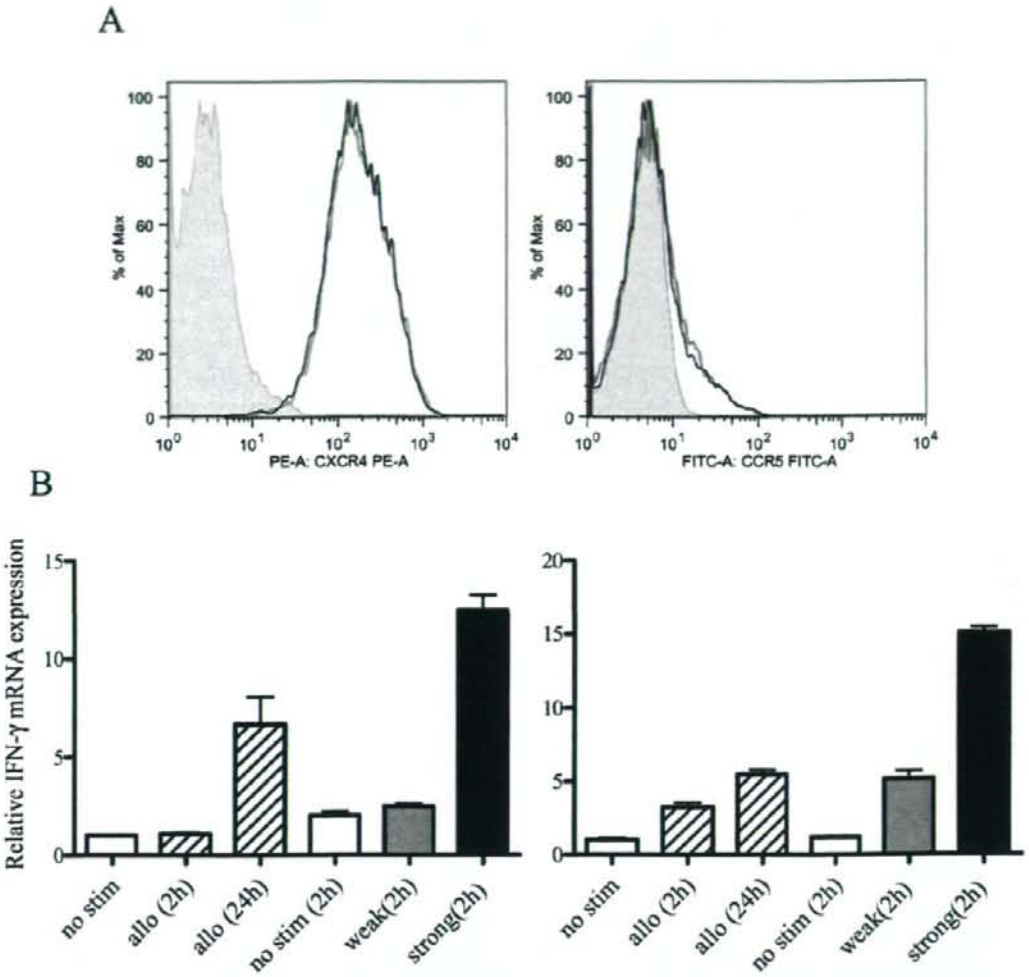

Figure 6. Analysis of CD4⁺ T cell activation. (A) Primary CD4⁺ T cells were stimulated with anti-CD3 (5 μg/ml)+anti-CD28 (10 μg/ml) (black bold line), anti-CD3 (0.5 μg/ml)+anti-CD28 (1 μg/ml) (black line), or cocultured with allogeneic CD4⁺ T cells for 2 h (gray line). Isotype control mAbs were used as a negative staining control (shaded peak). (B) One-step qRT-PCR analysis of IFN-γ mRNA expression in primary CD4⁺ T cells. Primary CD4⁺ T cells were cocultured with allogeneic CD4⁺ T cells for 2 or 24 h and then stimulated with anti-CD3 (5 μg/ml)+anti-CD28 (10 μg/ml) (IL-2 strong), anti-CD3 (0.5 μg/ml)+anti CD28 (1 μg/ml) (IL-2 weak), or no TCR stimulation (IL-2) for 2 h. Total RNA was extracted and analyzed by qRT-PCR. The data was normalized to EF-1α and the relative amount of IFN-γ is shown. The data represents the average ±SD of three independent experiments.
doi:10.1371/journal.ppat.1000279.g006

level of activation is enough for R5, but not for X4, to establish the viral life cycle. It is known that the retrovirus integration in a single cell is somehow limited process [45]. The CD4⁺ T cells may have come into contact with R5 and X4 HIV-1 produced by DCs with similar efficiency through the synapse, allowing the two variants to enter simultaneously into cells. However, once R5 HIV-1 is integrated in weakly activated CD4⁺ T cells, a delayed progression of X4 HIV-1 life cycle may be outcompeted by R5 HIV-1 even if the CD4⁺ T cells are later fully activated.

In summary, we visualized selective replication of the R5 HIV-1 variant following interactions between infected MDDCs and CD4⁺ T cells. We do not ascribe this to increased infectivity of R5 virus over X4 virus in MDDCs, but, rather, to the activation state of CD4⁺ T cells when they encounter a low level of these viruses at the infectious synapse. It is during antigen-specific interactions between DCs and CD4⁺ T cells that HIV-1 transmission occurs most efficiently *in vivo*, and it is during these interactions that R5 virus replicates preferentially over X4 virus.

Methods

Construction of plasmids

The plasmid pNL-E is a pNL432 (GenBank #M19921)-based proviral clone expressing EGFP, as described previously [32]. To create the pNL432-based proviral clone pNL-D, which expresses DsRed, a fragment of the DsRed gene, along with the pNL432 *env* region from the Hpa I digestion site to 3′ end of the *env*, was amplified by PCR, digested with Hpa I and Not I, and then ligated into the corresponding site in pNL-E. The EGFP and DsRed genes are located downstream of *env*, followed by an internal ribosome entry site (IRES) and *nef*.

To generate R5 tropic HIV-1, we constructed a proviral clone called pNLAD8-D by digesting pNL432-based pNLAD8 DNA (*env* is originated from HIV-1_{ADA} strain, kindly provided by Michael W. Cho, Department of Medicine, Case Western Reserve University School of Medicine, Cleveland, OH, USA, GenBank #AF004394) with BamHI and EcoRI and replacing X4 *env* with R5 *env* fragments.

Luc assay

1G5 or 1G5/CCR5 cells were infected with 50 ng of p24-measured amounts of HIV-1_{NL432}, HIV-$1_{NL\text{-}E}$, HIV-$1_{NL\text{-}D}$, or HIV-$1_{NLAD8\text{-}D}$ per 1×10^5 cells for 2 h, washing three times, and then culturied. After 48 h post-infection, cell lysates were prepared and the Luc assay was performed according to the manufacturer's instructions (Promega).

Preparation of HIV-1 virus stocks

To prepare HIV-1 virus stocks, human embryonic kidney cell line 293T cells were transfected with 20 μg of pNL432, pNL-E, pNL-D or pNLAD8-D using the calcium phosphate precipitation method and then incubation for 48 h. Culture supernatant was treated with benzonase (1 U/ml) for 30 min at 37°C, cleared by filtration, and then frozen at −80°C. The amount of virus in each culture supernatant was measured by in-house HIV-1 Gag p24 ELISA [17].

Cell culture

The 293T cells were maintained in Dulbecco's Modified Eagle Medium (Invitrogen [GIBCO], Carlsbad, CA, USA), supplemented with 10% heat-inactivated fetal bovine serum (FBS), penicillin (100 μg/ml), and streptomycin (100 μg/ml). 1G5 (obtained from AIDS Research and Reference Reagent Program, USA) and 1G5/CCR5 cells (CCR5 transfectants of 1G5 cells) were maintained in RPMI-1640 medium supplemented with 10% FBS, penicillin (100 μg/ml), streptomycin (100 μg/ml) (10% FBS-RPMI) and puromycin (2 μg/ml). CEMx174 CCR5/LTR-EGFP cells were maintained in RPMI-1640 medium supplemented with 10% FBS, penicillin (100 μg/ml), streptomycin (100 μg/ml) (10% FBS-RPMI), puromycin (2 μg/ml), and blasticidin (5 μg/ml) [36].

MDDC and T cells were prepared as described previously [46]. Blood samples were collected from healthy donors after we received written informed consent, and the collection was approved by the institutional ethical committee. The PBMCs were separated by a ficoll-hypaque density gradient (Lymphosepal: IBL, Gunma, Japan), enriched for $CD14^+$ cells with magnetic anti-CD14 beads and a magnetic cell sorter (MACS, Miltenyi Biotec, Cologne, Germany), and cultured for 7 d in the presence of 10 ng/ml IL-4 and 10 ng/ml GM-CSF (both from PeproTech London, United Kingdom). CD4+ T cells were negatively selected by depletion using the EasySep human $CD4^+$ T cell enrichment kit (StemCell Technologies, Vancouver, Canada). The purity of $CD4^+$ T cells was >98%, as assessed by FACScalibur (BD Biosciences, San Jose, CA, USA).

Kinetics of virus production in PHA blasts

PHA blasts were prepared by stimulating PBMCs with 5 μg/ml PHA and, 3 d later, infecting them with 20 ng of p24-measured amounts of HIV-1_{NL432}, HIV-$1_{NL\text{-}E}$, HIV-$1_{NL\text{-}D}$, or HIV-$1_{NLAD8\text{-}D}$ per 1×10^6 cells for 2 h, washing them three times, and then culturing them with 10% FBS-RPMI containing a recombinant interleukin-2 (IL-2) 50 U/ml. Culture supernatants were harvested at 3–4 d intervals and viral production was monitored by in-house HIV-1 p24 Gag antigen ELISA.

For flow cytometric analysis of fluorescent proteins, HIV-1-infected PHA blasts were stained with APC-labeled anti-CD3 mAb for 15 min on ice, washed once, and resuspended in staining buffer (PBS, 2% FBS, and 0.05% sodium azide) containing 1 μg/ml propidium iodide (PI). These cells were analyzed by FACScalibur using the Cell Quest program. The FACS data were reanalyzed using Flowjo software by gating live (PI-negative) $CD3^+$ T cells (Tree Star, San Carlos, CA, USA).

Quantitative PCR and RT-PCR analysis

HIV-$1_{NL\text{-}E^-}$ or $HIV_{NLAD8\text{-}D}$-infected MDDCs or $CD4^+$ T cells were collected and total DNA was prepared at 6 and 18 hpi. For the detection and quantification of individual forms of HIV-1 DNA, oligonucleotide primers and probe sequences were specifically designed for the TaqMan assay as described elsewhere [36]. All probes (Biosearch Technologies, Novato, CA, USA) were 5′ labeled with the fluorophore FAM as the reporter dye, and 3′ labeled with Black Hole Quencher-1 (BHQ-1) as the quencher dye. The amount of HIV-1–specific DNA per cell was normalized to that of the β-globin gene.

For allogeneic stimulation, primary $CD4^+$ T cells (1×10^6) were cocultured with allogeneic MDDCs (1×10^5) in 96-well round bottom plates for 2 or 24 h. The cells were then washed with PBS, and anti-CD11c mAb was added to half of the cells to deplete MDDCs from the DC–T cell coculture. After incubating for 15 min on ice, the anti-CD11c-reacted cells were incubated with Dynabead M450 goat anti-mouse IgG (Dynal Biotech, Lake Success, NY, USA) for 30 min at 4°C, and then $CD11c^+$ MDDCs were removed using a magnet stand. For TcR stimulation, primary $CD4^+$ T cells were left unstimulated, weakly stimulated with 0.5 μg/ml anti-CD3 and 1 μg/ml anti-CD28, or strongly stimulated with 5 μg/ml anti-CD3 and 10 μg/ml anti-CD28 for 2 h. Total RNA was extracted from these $CD4^+$ T cells, and qRT-PCR analysis was performed to measure the level of IFN-γ mRNA expression using the SuperScript III Platinum SYBR Green One-Step Quantitative RT-PCR system (Invitrogen). The sequences of the qRT-PCR primers were as follows: IFN-γ forward, 5′-tcccatgggttgtgtgttta-3′ and IFN-γ reverse 5′-aagcaccaggcatgaaatct-3′. The amount of IFN-γ mRNA was normalized to elongation factor 1 alpha (*EF-1α*) mRNA expression. The reaction was performed using an Mx3000P (Stratagene, La Jolla, CA, USA).

HIV-1 infection of MDDCs and transmission to $CD4^+$ T cells

MDDCs were left uninfected or were infected with 200 ng each of HIV-$1_{NL\text{-}E}$ and HIV-$1_{NLAD8\text{-}D}$ per 1×10^6 cells for 2 h, washed three times, and then cultivated for 24 h in 24-well culture plates. HIV-infected or mock-infected MDDCs were collected, washed with PBS, treated with 0.025% trypsin for 5 min at 37°C, and then washed twice with 10% FBS-RPMI. MDDCs (0.5×10^5 per well) were cocultured with autologous or allogeneic $CD4^+$ T cells

(0.5×10^6 per well) in 96-well round-bottom plates. In some cases, purified protein derivatives of 25 μg/ml *Mycobacterium tuberculosis* (PPD) or a 10% final volume of CMV antigen (CMV_{AD169}-infected MRC-5 lysate, kindly provided by N. Inoue, The first department of Virology, National Institute of Infectious Diseases, Tokyo, Japan) were added to the culture. The $CD4^+$ T cells stimulated with the weak or strong IL-2 protocol, described above, were left uninfected or were infected with 200 ng each of HIV-1_{NL-E} and HIV-$1_{NLAD8-D}$ per 1×10^6 cells for 2 h, extensively washed, and cultivated in 48-well tissue culture plates (1×10^6 per well) in 10% FBS-RPMI containing IL-2. These culture supernatants were harvested at 3–4 d intervals, and viral production was monitored by p24 antigen ELISA.

For flow cytometric detection of R5 ($DsRed^+$) and/or X4 ($EGFP^+$) HIV-1-infected $CD4^+$ T cells, cells were stained with APC-labeled anti-CD3 mAbs, and PI^- $CD3^+$ cells were analyzed by FACScalibur using the Cell Quest program and reanalyzed using Flowjo software.

Acknowledgments

We thank our colleagues and K. Okano in the Department of Immunology, National Institute of Infectious Diseases, for their excellent technical assistance. We also thank B. Autran and V. Appay (Cellular Immunology Laboratory, INSERM U543, Paris, France) for valuable discussions. The following reagent was obtained through the AIDS Research and Reference Reagent Program, Division of AIDS, NIAID, NIH: 1G5 from Dr. Estuardo Aguilar-Cordova and Dr. John Belmont.

Author Contributions

Conceived and designed the experiments: TY YTY JiI. Performed the experiments: TY YTY YyM KT. Analyzed the data: TY YTY. Contributed reagents/materials/analysis tools: YTY FM TT YI NY KK. Wrote the paper: TY YTY.

References

1. Berger EA, Doms RW, Fenyo EM, Korber BT, Littman DR, et al. (1998) A new classification for HIV-1. Nature 391: 240.
2. Wolinsky SM, Wike CM, Korber BT, Hutto C, Parks WP, et al. (1992) Selective transmission of human immunodeficiency virus type-1 variants from mothers to infants. Science 255: 1134–1137.
3. Zhu T, Mo H, Wang N, Nam DS, Cao Y, et al. (1993) Genotypic and phenotypic characterization of HIV-1 patients with primary infection. Science 261: 1179–1181.
4. van't Wout AB, Kootstra NA, Mulder-Kampinga GA, Albrecht-van Lent N, Scherpbier HJ, et al. (1994) Macrophage-tropic variants initiate human immunodeficiency virus type 1 infection after sexual, parenteral, and vertical transmission. J Clin Invest 94: 2060–2067.
5. Roos MT, Lange JM, de Goede RE, Coutinho RA, Schellekens PT, et al. (1992) Viral phenotype and immune response in primary human immunodeficiency virus type 1 infection. J Infect Dis 165: 427–432.
6. Schuitemaker H, Koot M, Kootstra NA, Dercksen MW, de Goede RE, et al. (1992) Biological phenotype of human immunodeficiency virus type 1 clones at different stages of infection: progression of disease is associated with a shift from monocytotropic to T-cell-tropic virus population. J Virol 66: 1354–1360.
7. Tersmette M, Gruters RA, de Wolf F, de Goede RE, Lange JM, et al. (1989) Evidence for a role of virulent human immunodeficiency virus (HIV) variants in the pathogenesis of acquired immunodeficiency syndrome: studies on sequential HIV isolates. J Virol 63: 2118–2125.
8. Connor RI, Sheridan KE, Ceradini D, Choe S, Landau NR (1997) Change in coreceptor use coreceptor use correlates with disease progression in HIV-1-infected individuals. J Exp Med 185: 621–628.
9. Grivel JC, Margolis LB (1999) CCR5- and CXCR4-tropic HIV-1 are equally cytopathic for their T-cell targets in human lymphoid tissue. Nat Med 5: 344–346.
10. Li S, Juarez J, Alali M, Dwyer D, Collman R, et al. (1999) Persistent CCR5 utilization and enhanced macrophage tropism by primary blood human immunodeficiency virus type 1 isolates from advanced stages of disease and comparison to tissue-derived isolates. J Virol 73: 9741–9755.
11. Moore JP, Kitchen SG, Pugach P, Zack JA (2004) The CCR5 and CXCR4 coreceptors–central to understanding the transmission and pathogenesis of human immunodeficiency virus type 1 infection. AIDS Res Hum Retroviruses 20: 111–126.
12. Banchereau J, Steinman RM (1998) Dendritic cells and the control of immunity. Nature 392: 245–252.
13. Tsunetsugu-Yokota Y (2008) Transmission of HIV from dendritic cells to CD4+ T cells: a promising target for vaccination and therapeutic intervention. Nova Science Publishers: in press.
14. Tsunetsugu-Yokota Y, Akagawa K, Kimoto H, Suzuki K, Iwasaki M, et al. (1995) Monocyte-derived cultured dendritic cells are susceptible to human immunodeficiency virus infection and transmit virus to resting T cells in the process of nominal antigen presentation. J Virol 69: 4544–4547.
15. David SA, Smith MS, Lopez GJ, Adany I, Mukherjee S, et al. (2001) Selective transmission of R5-tropic HIV type 1 from dendritic cells to resting CD4+ T cells. AIDS Res Hum Retroviruses 17: 59–68.
16. Granelli-Piperno A, Delgado E, Finkel V, Paxton W, Steinman RM (1998) Immature dendritic cells selectively replicate macrophagetropic (M-tropic) human immunodeficiency virus type 1, while mature cells efficiently transmit both M- and T-tropic virus to T cells. J Virol 72: 2733–2737.
17. Tsunetsugu-Yokota Y, Yasuda S, Sugimoto A, Yagi T, Azuma M, et al. (1997) Efficient virus transmission from dendritic cells to CD4+ T cells in response to antigen depends on close contact through adhesion molecules. Virology 239: 259–268.
18. McDonald D, Wu L, Bohks SM, KewalRamani VN, Unutmaz D, et al. (2003) Recruitment of HIV and its receptors to dendritic cell-T cell junctions. Science 300: 1295–1297.
19. Wu L, KewalRamani VN (2006) Dendritic-cell interactions with HIV: infection and viral dissemination. Nat Rev Immunol 6: 859–868.
20. Koot M, van Leeuwen R, de Goede RE, Keet IP, Danner S, et al. (1999) Conversion rate towards a syncytium-inducing (SI) phenotype during different stages of human immunodeficiency virus type 1 infection and prognostic value of SI phenotype for survival after AIDS diagnosis. J Infect Dis 179: 254–258.
21. Meng G, Sellers MT, Mosteller-Barnum M, Rogers TS, Shaw GM, et al. (2000) Lamina propria lymphocytes, not macrophages, express CCR5 and CXCR4 and are the likely target cell for human immunodeficiency virus type 1 in the intestinal mucosa. J Infect Dis 182: 785–791.
22. Bleul CC, Wu L, Hoxie JA, Springer TA, Mackay CR (1997) The HIV coreceptors CXCR4 and CCR5 are differentially expressed and regulated on human T lymphocytes. Proc Natl Acad Sci U S A 94: 1925–1930.
23. Peng G, Greenwell-Wild T, Nares S, Jin W, Lei KJ, et al. (2007) Myeloid differentiation and susceptibility to HIV-1 are linked to APOBEC3 expression. Blood 110: 393–400.
24. Cavrois M, Neidleman J, Kreisberg JF, Fenard D, Callebaut C, et al. (2006) Human immunodeficiency virus fusion to dendritic cells declines as cells mature. J Virol 80: 1992–1999.
25. Pion M, Arrighi JF, Jiang J, Lundquist CA, Hartley O, et al. (2007) Analysis of HIV-1-X4 fusion with immature dendritic cells identifies a specific restriction that is independent of CXCR4 levels. J Invest Dermatol 127: 319–323.
26. Pierson T, McArthur J, Siliciano RF (2000) Reservoirs for HIV-1: mechanisms for viral persistence in the presence of antiviral immune responses and antiretroviral therapy. Annu Rev Immunol 18: 665–708.
27. Spina CA, Guatelli JC, Richman DD (1995) Establishment of a stable, inducible form of human immunodeficiency virus type 1 DNA in quiescent CD4 lymphocytes in vitro. J Virol 69: 2977–2988.
28. Vicenzi E, Bordignon PP, Biswas P, Brambilla A, Bovolenta C, et al. (1999) Envelope-dependent restriction of human immunodeficiency virus type 1 spreading in CD4(+) T lymphocytes: R5 but not X4 viruses replicate in the absence of T-cell receptor restimulation. J Virol 73: 7515–7523.
29. Popik W, Pitha PM (2000) Inhibition of CD3/CD28-mediated activation of the MEK/ERK signaling pathway represses replication of X4 but not R5 human immunodeficiency virus type 1 in peripheral blood CD4(+) T lymphocytes. J Virol 74: 2558–2566.
30. Cicala C, Arthos J, Martinelli E, Censoplano N, Cruz CC, et al. (2006) R5 and X4 HIV envelopes induce distinct gene expression profiles in primary peripheral blood mononuclear cells. Proc Natl Acad Sci U S A 103: 3746–3751.
31. Sirois M, Robitaille L, Sasik R, Estaquier J, Fortin J, et al. (2008) R5 and X4 HIV Viruses Differentially Modulate Host Gene Expression in Resting CD4(+) T Cells. AIDS Res Hum Retroviruses 24: 485–493.
32. Suzuki Y, Koyanagi Y, Tanaka Y, Murakami T, Minawa N, et al. (1999) Determinant in human immunodeficiency virus type 1 for efficient replication under cytokine-induced CD4(+) T-helper 1 (Th1)- and Th2-type conditions. J Virol 73: 316–324.
33. Aguilar-Cordova E, Chinen J, Donehower L, Lewis DE, Belmont JW (1994) A sensitive reporter cell line for HIV-1 tat activity, HIV-1 inhibitors, and T cell activation effects. AIDS Res Hum Retroviruses 10: 295–301.
34. Lore K, Smed-Sorensen A, Vasudevan J, Mascola JR, Koup RA (2005) Myeloid and plasmacytoid dendritic cells transfer HIV-1 preferentially to antigen-specific CD4+ T cells. J Exp Med 201: 2023–2033.
35. Smed-Sorensen A, Lore K, Vasudevan J, Louder MK, Andersson J, et al. (2005) Differential susceptibility to human immunodeficiency virus type 1 infection of myeloid and plasmacytoid dendritic cells. J Virol 79: 8861–8869.

36. Yamamoto T, Miyoshi H, Yamamoto N, Yamamoto N, Inoue J, et al. (2006) Lentivirus vectors expressing short hairpin RNAs against the U3-overlapping region of HIV nef inhibit HIV replication and infectivity in primary macrophages. Blood 108: 3305–3312.
37. Rinaldo CR, Jr, Piazza P (2004) Virus infection of dendritic cells: portal for host invasion and host defense. Trends Microbiol 12: 337–345.
38. Rescigno M, Urbano M, Valzasina B, Francolini M, Rotta G, et al. (2001) Dendritic cells express tight junction proteins and penetrate gut epithelial monolayers to sample bacteria. Nat Immunol 2: 361–367.
39. Bomsel M (1997) Transcytosis of infectious human immunodeficiency virus across a tight human epithelial cell line barrier. Nat Med 3: 42–47.
40. Meng G, Wei X, Wu X, Sellers MT, Decker JM, et al. (2002) Primary intestinal epithelial cells selectively transfer R5 HIV-1 to CCR5+ cells. Nat Med 8: 150–156.
41. Bobardt MD, Chatterji U, Selvarajah S, Van der Schueren B, David G, et al. (2007) Cell-free human immunodeficiency virus type 1 transcytosis through primary genital epithelial cells. J Virol 81: 395–405.
42. Hu J, Gardner MB, Miller CJ (2000) Simian immunodeficiency virus rapidly penetrates the cervicovaginal mucosa after intravaginal inoculation and infects intraepithelial dendritic cells. J Virol 74: 6087–6095.
43. Spira AI, Marx PA, Patterson BK, Mahoney J, Koup RA, et al. (1996) Cellular targets of infection and route of viral dissemination after an intravaginal inoculation of simian immunodeficiency virus into rhesus macaques. J Exp Med 183: 215–225.
44. Stevenson M (2003) HIV-1 pathogenesis. Nat Med 9: 853–860.
45. Chattopadhyay S, Rowe WP, Levine AS (1976) Quantitative studies of integration of murine leukemia virus after exogenous infection. Proc Natl Acad Sci U S A 73: 4095–4099.
46. Tsunetsugu-Yokota Y, Morikawa Y, Isogai M, Kawana-Tachikawa A, Odawara T, et al. (2003) Yeast-derived human immunodeficiency virus type 1 p55(gag) virus-like particles activate dendritic cells (DCs) and induce perforin expression in Gag-specific CD8(+) T cells by cross-presentation of DCs. J Virol 77: 10250–10259.

ELSEVIER

INSTITUT PASTEUR

Microbes and Infection 11 (2009) 191–197

www.elsevier.com/locate/micinf

Original article

Activation of HIV-1 Gag-specific CD8$^+$ T cells by yeast-derived VLP-pulsed dendritic cells is influenced by the level of mannose on the VLP antigen

Fuminori Mizukoshi [a], Takuya Yamamoto [a], Yu-ya Mitsuki [a], Kazutaka Terahara [a], Ai Kawana-Tachikawa [b], Kazuo Kobayashi [a], Aikichi Iwamoto [b], Yuko Morikawa [c], Yasuko Tsunetsugu-Yokota [a,*]

[a] *Department of Immunology, National Institute of Infectious Diseases, Toyama 1-23-1 Shinjuku-ku, Tokyo, Japan*
[b] *Department of Infectious Diseases, Institute of Medical Science, University of Tokyo, Shirokanedai 4-6-1, Minato-ku, Tokyo, Japan*
[c] *Kitasato Institute for Life Sciences and Graduate School for Infection Control, Kitasato University, Shirokane 5-9-1, Minato-ku, Tokyo, Japan*

Received 3 October 2008; accepted 12 November 2008
Available online 24 November 2008

Abstract

Dendritic cells (DCs) are professional antigen-presenting cells that possess a unique capacity to cross-present exogenous antigens efficiently to CD8$^+$ T cells. We previously demonstrated that monocyte-derived DCs (MDDCs) pulsed with yeast-derived HIV-1 Gag virus-like particles (VLPs) were able to activate Gag-specific CD8$^+$ T cells from HIV-1-infected individuals. Yeast VLPs are abundantly mannosylated (high-mannose type: HmVLPs) and are highly immunogenic. Because lectin receptors are shown to negatively regulate Th1 responses, we investigated the relationship between VLP mannosylation level and MDDC cross-presentation activity. Poorly mannosylated VLPs (low-mannose type: LmVLPs) were prepared using a yeast mnn9 mutant strain that lacks a core mannosylation enzyme. We found that MDDCs pulsed with LmVLPs activated Gag-specific T cells more strongly than those pulsed with HmVLPs. However, MDDCs showed similar antigen uptake and intracellular transport of both types of VLPs. Interestingly, LmVLPs induced IL-12 production slightly more than HmVLPs (yet statistically significant). Furthermore, the level of LPS-induced IL-10 production was enhanced by pulsing with HmVLPs, but not with LmVLPs. These results indicate that lectin receptors recognizing mannose may influence the Th1/Th2 balance of the immune response, resulting in reduced efficiency of CD8$^+$ T cell activation by a heavily mannosylated antigen presented by DCs.

Keywords: Antigen presentation; Mannosylation; AIDS

1. Introduction

Dendritic cells (DCs) are professional antigen-presenting cells that play a pivotal role in the immune system by acting as "sentinel cells" [1]. DC-based immunotherapy has been developed to treat a variety of diseases, including cancer [2,3], autoimmune diseases [4], transplant rejection [5], allergic diseases [6], and infectious diseases [7]. Previous studies of human immunodeficiency virus (HIV) and simian immunodeficiency virus (SIV) infections demonstrated that monocyte-derived DCs (MDDCs) pulsed with inactivated viruses enhanced both cellular and humoral immune responses [8,9]. However, the efficacies of DC-based immunotherapy for clinical applications have been inconsistent, probably because of the different protocols for cultivating and maturating the DCs, for the selection and loading of antigens, and for the administration, route, dose, and frequency of the therapy.

* Corresponding author: Tel.: +81 3 5285 1111x2133; fax: +81 3 5285 1150 or 1156.
E-mail address: yyokota@nih.go.jp (Y. Tsunetsugu-Yokota).

1286-4579/$ - see front matter
doi:10.1016/j.micinf.2008.11.004

Acquired immune deficiency syndrome (AIDS), which is caused by HIV infection, is an enormous public health threat worldwide. The development of highly active anti-retroviral therapy (HAART) has markedly improved treatment of HIV-infected individuals and has significantly reduced HIV-associated mortality [10]. However, HAART cannot completely eradicate HIV [11]. Therefore, a novel strategy is required for treating HIV infections.

In terms of the host immune response against HIV, antigen-specific $CD8^+$ cytotoxic T lymphocytes (CTLs) are known to be important in suppressing HIV replication [12]. Therefore, CTL-inducible vaccines have been developed, most of them virus-based [13]. We previously showed that DCs pulsed with yeast-derived HIV-1 Gag virus-like particles (VLPs) activated Gag-specific T cells *in vitro* [14]. Because VLPs are neither infectious nor replicative, and also can be easily produced on a large scale, a VLP-based vaccine is an excellent candidate for a vaccine based on cross-presentation.

Highly glycosylated antigens have strong immunogenicity, whether expressed by yeast or using a baculoviral system. For example, mannosylation of antigens augments antigen-specific T cell responses [15,16]. However, recent studies revealed that the stimulation of lectin receptors on DCs induced interleukin (IL)-10 production, resulting in a shift in immune regulation towards Th2 dominance [17–19]. Thus, the influence of carbohydrate chains on the immune response is a concern for novel vaccine developments.

We postulated that the cross-presentation activity of DC is influenced by the degree of antigen mannosylation. In this study, we compared the antigenicity of abundantly mannosylated VLPs derived from a wild-type yeast to that of poorly mannosylated VLPs derived from a yeast mnn9 mutant lacking mannosylating enzyme.

2. Materials and methods

2.1. Preparation of cells

Fresh peripheral blood mononuclear cells (PBMCs) were obtained from healthy donors by Ficoll density gradient centrifugation. $CD14^+$ cells were positively isolated from PBMCs using a MACS system (Miltenyi Biotech, Bergisch Gladbach, Germany) according to the manufacturer's protocol. We generated immature MDDCs using 10 ng/ml human granulocyte-macrophage colony-stimulating factor and 20 ng/ml IL-4 as previously described [14]. These blood samples were collected with written informed consent under the approval of the ethical committee in National Institute of Infectious Diseases (NIID).

A Gag28 peptide (p17:KYKLKHIVW)-specific CTL line was established from PBMCs of HIV-1-infected individuals carrying HLA-A*2402 as previously described [20]. The studies utilizing PBMCs of HIV-infected patients were approved by the ethical committees in NIID and the Institute of Medical Science (University of Tokyo), and PBMCs were collected with written informed consent.

2.2. Production and purification of yeast-derived HIV-1 Gag VLPs

Wild-type yeast-derived VLPs from HIV-1 Gag, VLPs fused with green fluorescent protein (EGFP) and control culture supernatant (CS) were produced as described previously [14,21]. The mutant *S. cerevisiae* mnn9 strain [22] was used to produce low mannose-type VLPs. Standard purification and sucrose density gradient analysis of Gag VLPs was performed as described previously [23]. Purified VLPs were obtained by fractionation of the gradients. For comparison, *Spodoptera frugiperda* (*Sf9*) cells were infected with recombinant *Autographa californica* nuclear polyhedrosis viruses (baculoviruses) containing the full-length HIV-1 *gag* gene [23]. Purified Gag VLPs were quantitated by Coomassie brilliant blue staining. Total yeast protein was quantified by Bradford's method [21].

2.3. Quantitative analysis of mannose on the VLPs with dot blot technique

The samples were diluted with PBS and applied to a nitrocellulose membrane (0.45 μm pore size; GE Osmonics Labstore, Minnetonka, MA) using BioDot SF microfiltration apparatus (BioRad, Hercules, CA) according to the manufacturer's instructions. The membrane was soaked three times in blocking buffer (10 mM Tris–HCl pH 7.4, 0.15 M NaCl, 0.05% Tween20) for 10 min at room temperature (RT), then reacted with the biotinylated ConA (EY Laboratories, Inc., San Mateo, CA) (10 μg/ml in blocking buffer) for 90 min. After washing three times with blocking buffer, the membrane was incubated for 30 min at RT with horseradish peroxidase (HRP)-conjugated streptavidin (Boehringer-Roche, Basel, Switzerland) (1:5000 dilution). The SuperSignal West Dura kit (Pierce, Rockford, IL) was used for detection and the signal was analyzed by LAS-3000 (Fujifilm, Tokyo, Japan). The luminescence intensity of each dot was measured using Image Gauge densitometry software (version 4.0; Fujifilm).

2.4. Endocytosis assay

Immature MDDCs were incubated with various concentrations of CS or high- or low-mannose type VLP-EGFP at 37 °C for 3 h. These cells were washed extensively with flow cytometry (FCM) buffer (2% v/v fetal bovine serum and 50 μg/ml sodium azide in PBS), and resuspended in FCM buffer containing propidium iodide. The uptake of VLP-EGFP was quantified by measuring the fluorescence intensity using FACScalibur and CellQuest software (Becton Dickinson, Labware, NJ). For the receptor blocking assay, immature MDDCs were pre-cultured for 30 min in the presence of mAb against dendritic cell-specific intracellular adhesion molecule-3-grabbing nonintegrin (DC-SIGN) (10 μg/ml; eBioscience, San Diego, CA), mannose receptor (MR) mAb (10 μg/ml; BD Bioscience, Flanklin Lakes, NJ), mannan (2 mg/ml; Sigma–Aldrich) or isotype control IgG_{2a} (10 μg/ml; eBioscience), then pulsed with VLPs (10 μg/ml) or fluorescein-isothiocyanate

(FITC)-conjugated mannosylated BSA (man-BSA; Sigma–Aldrich) (100 μg/ml).

2.5. Subcellular fractionation and Western blotting analysis

Immature MDDCs cultured with 40 μg/ml of high- or low-mannose type VLPs were washed with PBS and then fractionated into cytosol and membrane/organelle fractions using ProteoExtract subcellular proteome extraction kit (Calbiochem, Darmstadt, Germany).

For Western blotting, cells or subcellular fractions were resuspended in lysis buffer (10 mM Tris–HCl pH 7.4, 150 mM NaCl, 1% sodium deoxycholate, 1% Triton X-100, 0.1% sodium dodecyl sulfate, 357.5 mM 2-mercaptoethanol). The lysate, containing 2×10^5 cells, was analyzed by 12.5% SDS-PAGE and electrophoretically transferred to a PVDF transfer membrane (Amersham Biosciences, Buckinghamshire, UK). Non-specific binding was blocked with washing buffer (10 mM Tris–HCl, 150 mM NaCl, 0.05% Tween 20) containing 3% skim milk for 30 min at RT. After washing, the membrane was stained for 1 h at RT either with the anti-Calpain mAb (Calbiochem) as a cytosolic marker or anti-gastrin-releasing peptide (GRP) 78 mAb (BD Bioscience) as a membrane/organelle marker. Subsequently, the membrane was incubated with biotin-conjugated anti-mouse IgG for 1 h at RT, followed by streptavidin-conjugated HRP (Boehringer-Roche) for 30 min at RT. Gag p24 was detected by incubation with HRP-conjugated anti-HIV Gag mAbs (clone 10B5; kindly provided by T. Sata, Department of Pathology, NIID, Tokyo, Japan) [24] for 1 h at RT. The immunoreactive bands were detected with SuperSignal West Dura kit and visualized by Lumino analyzer LAS-3000.

2.6. Detection of cytokines

To detect IFN-γ production, an enzyme-linked immunospot (ELISPOT) assay was carried out as previously described [14]. The culture supernatant was collected and the level of cytokines was measured with the cytometric beads array kit (BD Bioscience) according to the manufacturer's protocol.

3. Results

3.1. Characterization of VLPs generated from yeast mutant mnn9

To determine whether the level of antigen mannosylation can modulate the immune response, we generated VLPs from wild-type yeast and from the mannosyltransferase mutant mnn9. The mnn mutants are mostly defective in polymerization enzymes related to the synthesis of the outer chain portion of N-linked oligosaccharides, and the mnn9 strain is defective in the core enzyme for glycosylation [25]. The wild-type yeast-derived VLPs are heavily mannosylated and are designated as high-mannose type VLPs (HmVLPs); in contrast, mnn9 mutants produce poorly mannosylated VLPs (low-mannose type VLPs: LmVLPs). The mannosylation level of LmVLPs is considered to be more similar to the level of mannose on mammalian mannoproteins than that of HmVLPs.

Using sucrose density gradient analysis, HmVLPs were recovered mainly at the density of 1.210 g/ml (Fig. 1A, upper panel), while the major peak density of LmVLPs was at 1.196 g/ml (Fig. 1A, middle panel) and the major peak of baculovirus-based VLPs was at 1.180 g/ml (Fig. 1A, lower panel). Thus, the LmVLPs are smaller in size than HmVLPs, probably due to the lower degree of mannosylation.

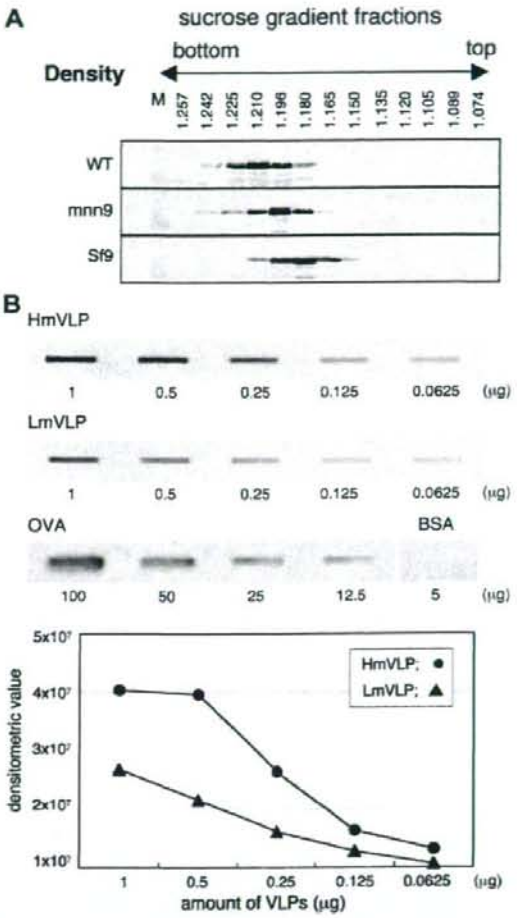

Fig. 1. Characterization of yeast VLPs. (A) Sucrose density gradient fractions were analyzed by Western blotting using anti-Gag mAbs. (Upper panel) HmVLPs derived from wild-type *S. cerevisiae* (WT). (Middle panel) LmVLPs derived from mnn9 mutant strain (mnn9). (Lower panel) VLPs derived from Sf9. 40 μg of VLPs were applied per assay, respectively. (B) Lectin staining was carried out on using biotinylated ConA and HRP-conjugated avidin. The number is indicative of the volume of sample applied per slot. The densitometric value of HmVLPs (filled circle) or LmVLPs (filled triangle) was measured by the computerization.

We next estimated the level of the mannosylation on these VLPs using lectin blot. In comparison with the LmVLPs generated from the mnn9 mutants, HmVLPs generated from a wild-type yeast strain clearly showed higher levels of mannose (Fig. 1B). As control, no mannose was detected in native BSA, while OVA was highly mannosylated. These results indicate that LmVLPs and HmVLPs differ in their mannose glycosylation levels.

3.2. The effect of uptake and intracellular dynamics of HmVLPs and LmVLPs

We first studied the internalization efficiency of EGFP-fused VLPs by MDDCs. We titrated the uptake of these VLPs at various concentrations (5–20 μg/ml). Both VLPs were taken up by MDDCs in a dose-dependent manner (Fig. 2A, upper panels), although the uptake of HmVLP was slightly better than that of LmVLP at 5 μg/ml.

In order to understand the mechanism of uptake of these VLPs by MDDCs, we carried out the blocking experiment. The uptake of these HmVLP and LmVLP at 10 μg/ml was strongly inhibited by mannan, but neither by anti-MR nor by anti-DC-SIGN mAbs (Fig. 2A, lowest panels). In contrast, the uptake of a high dose of man-BSA was remarkably inhibited by the same concentration of anti-MR, but not by anti-DC-SIGN mAb. Therefore, MDDCs are able to take up these VLPs at a similar level, probably by the mannose-mediated mechanism, but neither via DC-SIGN nor MR.

For cross-presentation of VLPs, the antigens incorporated in MDDCs have to be transported into the cytosol and processed by the proteasomes. To test whether the intracellular transport of VLPs is influenced by their level of mannosylation, the MDDCs were pulsed for 1 or 6 h with the

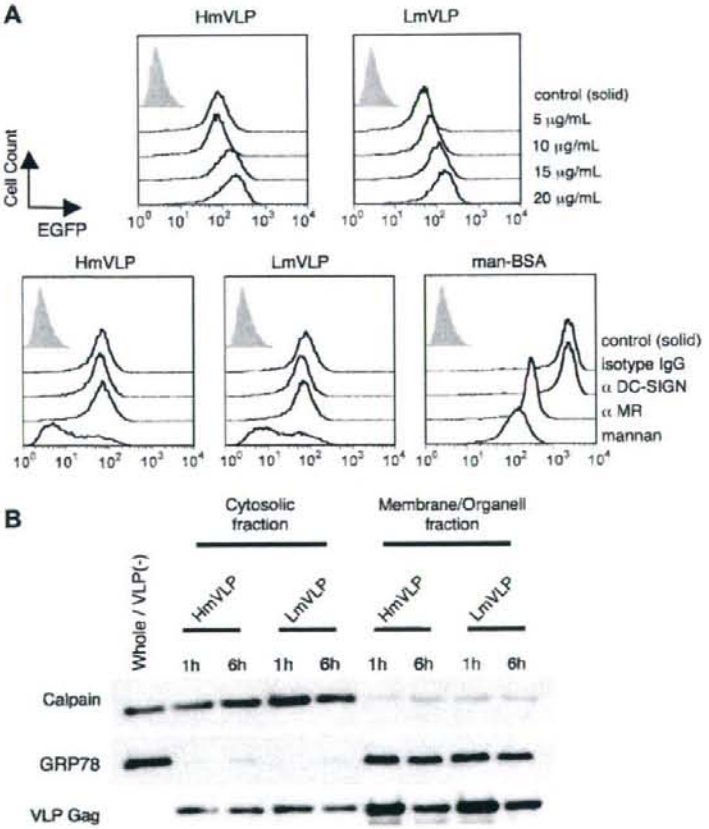

Fig. 2. Uptake and localization of yeast VLPs by DCs. (A) Immature MDDCs (5×10^4 cells/50 μl) were incubated with HmVLP-EGFP or LmVLP-EGFP (upper panel, indicated concentrations; lower panel, 10 μg/ml) for 3 h, analyzed by flow cytometry. Moreover, MDDCs were pre-incubated for 30 min with indicated antibodies (10 μg/ml) or mannan (2 mg/ml), and pulsed with HmVLP-EGFP or LmVLP-EGFP (10 μg/ml), mannosylated BSA (100 μg/ml) as a control (lower panel). The background signal is shown as a shadow. (B) Immature MDDCs (1×10^6 cells/200 μl) were incubated with 40 μg/ml yeast HmVLPs, LmVLPs or CS for 1 or 6 h, and fractionated. Whole cell lysate [Whole/VLP(−)] and cytosolic and membrane/organelle fractions were analyzed by Western blotting using antibodies against the cytosolic marker Calpain, the membrane marker GFP78, and VLP Gag.